CHARACTERIZATION OF RICE HUSK ASH WITH SPECIAL EMPHASIS ON MERCURY POROSIMETRY

By
K. MANOKARAN

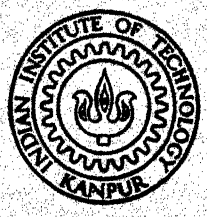

DEPARTMENT OF METALLURGICAL ENGINEERING
INDIAN INSTITUTE OF TECHNOLOGY KANPUR
AUGUST, 1983

CHARACTERIZATION OF RICE HUSK ASH WITH SPECIAL EMPHASIS ON MERCURY POROSIMETRY

A Thesis Submitted
in Partial Fulfilment of the Requirements
for the Degree of

MASTER OF TECHNOLOGY

By

K. MANOKARAN

to the

DEPARTMENT OF METALLURGICAL ENGINEERING

INDIAN INSTITUTE OF TECHNOLOGY KANPUR

AUGUST, 1983

ME - 1983 - M - MAN - CHA

To

My Parents

CERTIFICATE

This is to certify that this work entitled "CHARACTERIZATION OF RICE HUSK ASH WITH SPECIAL EMPHASIS ON MERCURY POROSIMETRY" by K. Manokaran has been carried out under my supervision and has not been submitted elsewhere for a degree.

Dr. P. C. Kapur
Professor
Department of Metallurgical Engineering
Indian Institute of Technology
Kanpur.

Kanpur
August 23, 1983.

ACKNOWLEDGEMENTS

I am deeply indebted to Professor P.C.Kapur for his invaluable guidance, constructive criticism and constant encouragement throughout the course of this work.

I am very thankful to Messrs R.K. Prasad, O.P. Malaviya and B. Sharma for their assistance throughout the experimental work.

My sincere thanks are due to Mr. V. Vijaya Bhaskar for having done the BET surface area analysis at the Univ. of California, Berkeley and Mr. P.K. Singh for the help rendered in various ways.

I also wish to thank Mr.M.R. Nathwani and Mr. S.J. Gupta for their efficient typing of this thesis.

Finally, I would like to express my gratitude to all my friends who made my stay here, at IIT Kanpur a memorable one.

CONTENTS

LIST OF FIGURES

ABSTRACT

Rice husk ash, a highly porous and siliceous material, has many applications, e.g. in the manufacture of cement, refractory, high thermal insulation, silicon carbide and nitride, solar grade silicon, and as fillers, filters etc. Properties of rice husk ash based products depend primarily on the nature of rice husk ash which is a function of its burning temperature. The rice husk burnt at 450, 600, 800, 1000, 1200 and 1400°C has been characterized for its microstructure and the related physical properties:

a) Density - Bulk and Apparent true density
b) X-ray Analysis
c) Surface Area by BET
d) Pore structure by Hg porosimetry (Main component of this work)
e) Liquid limit for field tests of rice husk ash reactivity.

In all these studies, a similar trend has been observed. The results are consistent and give a coherent pattern of the microstructure of rice husk ash. The tapped bulk and apparent true density values increase from 0.29 and 1.975 to 0.345 gm/cm^3 and 2.35 gm/cm^3 respectively over the temperature range 450 to 1400°C. The crystalline quartz phase starts forming at 550°C, but disappears as the temperature is increased to 1000°C. The

crystobalite phase appears at 800°C and the amount increases with increase in temperature. In 1000, 1200 and 1400°C fired husk ash samples the crystobalite and tridymite phases are coexisting. The porosity decreases from 41% to 13.25% and the specific surface areas measured both by Hg-porosimetry and BET decrease rapidly from 38.12 and 76 to 0.975 and 0.12 m^2/g respectively over the temperature range 600 to 1200°C. A bimodal distribution of pores is observed in all the fired rice husk ash samples. Liquid limit tests show a remarkable drop in the liquid limit between 600 and 1000°C consistent with porosity, surface area and x-ray analysis.

CHAPTER 1

INTRODUCTION

The present work deals mainly with characterization of the microstructure and related physical properties of Rice Ash burnt at different temperatures, with special emphasis on elucidation of its pore structure by mercury porosimetry.

Rice Husk Ash, obtained by burning Rice Husk, an agricultural waste material and a nuisance by product, is highly porous and mostly silica. This facinating and valuable source of bio-silica can yield a variety of useful silica based products. It possesses cementing, refractory, high temperature insulation and filler properties.

The fully burnt Ash contains about 95% silica and is highly porous in nature. It can be reacted with Alumina in stoichiometric proportions to give porous mullite[1], a valuable thermal insulation. With lime it is used to prepare hydraulic setting cement called Ashmoh[2,3]. It can be bonded with ordinary portland cement in predetermined proportions to give Ashment cement[2,4] which is superior to portland cement in some respects, specially its high corrosion resistance. By reacting Rice Husk Ash with sintered magnesite high insulating refractory called fosterite[5] can be produced. Straight silica insulating refractories can also be prepared by

bonding Rice husk Ash with calcium ferrites or sodium silicate[5]. Silicon carbide[6] an important material in the field of non-oxide refractories and abrasives can be made at relatively low temperatures from Rice Husk. Recent developments have shown that solar grade polycrystalline silicon[7] of reasonably good quality (better than 99.9% purity) could be produced economically from Rice Husk Ash by reduction with magnesium.

The properties of the products from Rice husk Ash depend mainly on the physical-chemical nature of Rice Husk Ash, which in-turn is a function of burning temperature of rice husk. Depending on time and temperature of burning or combustion the silica in ash remains either in an amorphous phase or is transformed into its various polymorphic modifications namely quartz, tridymite and crystobalite. These forms of silica differ in their physical and chemical properties such as density, hardness, surface area, pore structure and chemical reactivity.

Since the surface area and the porous structure of rice husk ash play an important role in all its utilization, an attempt has been made to characterize the pore structure and reactivity of ash as a function of its combustion temperature. The samples of rice husk ash were fired at different tempera-

tures ranging from 450°C to 1400°C in an electric muffle furnace and also in TIB husk burner.

These ash samples were studied for:

i) Bulk and true densities

ii) Amorphous and crystalline nature of silica by x-ray diffraction technique

iii) Specific surface area by BET analysis.

iv) Surface area, cumulative pore volume and pore size distributions by mercury penetration porosimetry, which was the principal area of investigation.

iv) For quick and easy assessment of the reactivity of rice husk ash a simple field test has been developed which is based on determining the liquid limit at moist/plastic state of ash powders.

CHAPTER 2

LITERATURE REVIEW

2.1 Rice Husk and Rice Husk Ash:

Worlds production of rice paddy exceeds 400 Million tonnes per year currently out of which about 120 million tonnes is produced in china, 80 million tonnes in India and about 10-15 million tonnes each in Japan, Bangladesh, Indonesia, Thailand, Vietnam and Burma. Since the crop is widely spread in the Asian countries, the research effort has been concentrated in these countries.

Nature has provided the rice grain with a tough siliceous woody outer coat called rice hull or husk for protection in the course of its maturity. The husk which constitutes roughly 20 to 25% by weight of harvested paddy is split into two halves at the dehusking stage of rice milling operation. Rice Husk is 4 to 5 mm in length, 1 to 2 mm in width and about 0.5 mm thick. Its bulk density is very low 95 to 150 kg/m^3. Depending on the paddy strain soil and climate conditions and the agricultural practices employed the composition of rice husk varies slightly (Table 1).

The heat derived from the combustion of rice husk is of the order of 3×10^6 J/kg which is equivalent to about one

half of the calorific value of good quality coal. In some places husk is utilised as fuel for rice mill boilers and in most other places it is piled up in heaps in open fields and periodically set on fire to get rid of.

Harvested paddy yields for about 20-25% of husk which on burning leaves behind about 20% Ash. This Ash is mostly silica (95% +) which is originally present in hydrated opaline state, in the cellulose structure of rice husk. The nature and porosity of silica depend on temperature and time of burning/combustion and also the impurities present in ash. The refractoriness of the various silica based products depend primarily on its Alkali contents. The loose and tapped bulk densities of rice husk are 210 to 300 kg/m^3 and 280 to 400 kg/m^3. Typical compositions of rice husk and rice husk ash are shown in table 1[8].

2.2 Structure of Rice Husk Ash:

The phase changes in rice husk ash silica with temperature have been reported by Hanafi et al[9]. Silica samples were prepared by firing rice husk at various temperatures ranging from 500 to 1400°C at 100°C interval for 3 hours. The crystalline changes were detected by x-ray diffraction analysis. It is reported that no crystalline

TABLE 2.1

Chemical Analysis of Rice Husk and Rice Husk Ash

Rice Husk	wt%	Rice Husk Ash	wt%
Ash	16-25	SiO_2	87-97
Carbon	38-42	K_2O	0.6-2.5
Hydrogen	4.5-5.5	Na_2O	trace-1.75
Nitrogen	0.3-2.0	CaO	0.2-1.5
Sulphur	0.07-0.12	MgO	0.1-1.95
Oxygen	30-32	Fe_2O_3	trace-0.55
Moisture	rest	P_2O_5	0.5-2.80

modification was observed on heating rice husk upto 800-900°C. At 900°C the nucleation process for the formation of the low form of crystobalite phase pronounced. At 1000°C a sharp increase in the crystalline size of the silica grain was observed. The tridymite phase began to crystallise on heating to 1200°C. Whereas at 1300 and 1400°C the well ordered hexagonal form made its appearance alongwith the crystobalite.

Hanafi et al (9) have also shown the differential scanning calorimetric thermogram for the ash sample fired at 1200°C for 3 hours. According to these authors an exothermic peak

at 135°C represented the transformation of the tridymite ($T_{\beta} - T_{\alpha}$) and four peaks located at 190, 220, 235 and 250°C were due to the transformation of crystobalite phase ($C_{\alpha} - C_{\beta}$); the endotherms located at 190, 220 and 235°C represented the transformation of the low form of unordered crystobalite, whereas the endotherm located at 250°C represented the transformation of the well ordered crystalline form. Using infra red spectroscopy Ibrahim et al[10] have supported the Hanafi's theory of crystallisation of rice husk ash.

Vijaya Bhaskar[1] has characterized by x-ray, the rice husk ash samples heat treated at different temperatures for their crystalline nature and reported that the 350°C was mainly amorphous silica and a very small amount of quartz as opposed to the work of Hanafi and Ibrahim who reported no signs of quartz at any temperature range. Bhaskar further reported that without any change in the amount of quartz the crystobalite phase appeared first at 800°C and at 1000°C. Besides these two phases tridymite also started forming. Thereafter the quartz phase disappeared in 1200°C fired sample and the intensity of the tridymite phase increased.

The variation of density of rice husk ash with its combustion temperature was also carried out by Bhaskar. He found that specific gravity varied from 2.14 gm/cm^3 to

2.38 gm/cm^3. He explained the variation in terms of phase changes in silica, presence of small amounts of unburnt carbon trapped in the matrix, the fine enclosed pores present, the thermal history and impurities in the ash.

Hanafi et al[9] have reported BET surface area of rice husk ash combusted at different temperatures. It dropped from 200 m^2 g^{-1} for 500°C sample to 112 m^2 g^{-1} for 1000°C sample, increased to 147 m^2 g^{-1} in the ash fired to 1100°C again fell to 51 m^2 g^{-1} at 1300°C and rose to 146 m^2 g^{-1} at 1400. Not only the initial surface area values are too high, the authors do not explain the erratic results obtained by them. Their data seem to be suspect. It is however clear that the porosity and surface area of rice husk ash undergo drastic reduction with increase in combustion temperature. No detailed pore size distribution data on rice husk ash has been reported in the literature.

2.3 Mercury Porosimetry:

The special accent of this work was to study the the pore structure of ash by mercury porosimetry. Since the publication on mercury porosimetry in 1921[11], it is used as a standard tool to determine the size and quantity of void spaces and pores in porous materials and the density of both solid objects and powders in catalysts[12], coals[13],

rocks[14], ceramics[15], polymers[16] etc. In addition one can calculate specific surface area and obtain a measure of pore size distribution. Finally mercury expelled from pores as a function of decreasing pressure i.e. in the retraction curve, gives information about the shape and structure of pores.

Hg - porosimeter instrument indicates the quantity of a non-wetting liquid (e.g. mercury) that can be forced under a given pressure into the pores of the material in question and into the void spaces among particles. Any time a liquid exhibits a contact angle with a solid greater than 90° it will resist wetting the solid, entering into void spaces about it, or penetrating its pores. Mercury exhibits a greater contact angle with most materials than any other conveniently usuable liquid. Hence it is most suitable for the evaluation of voids and pore sizes.

Assuming circular cross section of voids or pores, the pressure and pore or void size relationship is

$$Pr = 2 \gamma \cos\theta \qquad (1)$$

where P is the applied pressure

r is the pore/void radius

γ is the surface tension of mercury

and θ is the contact angle of mercury

This equation shows that no pores or void spaces are penetrated by a non-wetting liquid mercury at zero pressure. As the pressure increases the quantity of liquid forced into the pores increases in proportion to the differential pore volume, the size of the pores corresponds to the instantaneous pressure.

Taking γ = 474 dynes cm^{-1} and $\theta = 130°$, the pore radius from eqn. (1) becomes

$$r = \frac{609 \times 10^4}{P \text{ (dynes cm}^{-2}\text{)}} = \frac{609 \times 10^3}{P \text{ (Pascal)}} = \frac{6.1}{P \text{ (kg cm}^{-2}\text{)}} \qquad (2)$$

Pressure penetration - volume curves can be utilized to calculate the specific surface area and pore size distribution of a powder with fair reliability provided sufficiently high pressures are applied to force mercury into the smallest pores.

The specific surface area is computed from[17]

$$S = - \frac{P \, dV}{\gamma \cos \theta} \qquad (3)$$

where dV is the volume of mercury forced into the pores of the powder by the external pressure P.

Taking γ = 474 dynes cm^{-1} and $\theta = 130°$ at 25°C

The specific surface area from eqn. (3) becomes

$$S = 0.0225 \int_0^{V_{max}} P \, dV \qquad (4)$$

The pore size distribution function(17) is given by

$$D(r) = \frac{P}{r} \frac{dV}{dp} \qquad (5)$$

dV is the volume of pores of radii between r and r + dr and

dp is the corresponding pressure difference

D(r) is graphically given by the slope of the V versus P plot.

2.4 Standard Liquid Limit Tests:

Atterberg limits or consistancy limits are the standard water limit tests in soil mechanics used to grade the soil or clay regarding its degree of firmness and the water absorption capacity[18]. The limits are the water contents at which the soil mass passes from one state to the next. The Atterberg limits which are most useful for engineering purposes are liquid limit, plastic limit and shrinkage limit. These limits are expressed as percent water content.

Liquid limit is the water content corresponding to the arbitrary limit between liquid and plastic state of consistancy of a soil. It is defined as the minimum water content at which the soil is still in the liquid state but has a small shearing strength against flowing which can be

measured by standard available means.

Plastic limit is the water content corresponding to an arbitrary limit between the plastic and the semi-solid states of consistancy of a soil. It is defined as the minimum water content at which a soil will just begin to crumble when rolled into a thread approximately 3 mm in diameter.

Shrinkage limit is defined as the maximum water content at which a reduction in water content will not cause a decrease in the volume of a soil mass. It is the lowest water content at which a soil can still be completely saturated. The figure 2.1 shows the four states of consistancy with the appropriate consistancy limits.

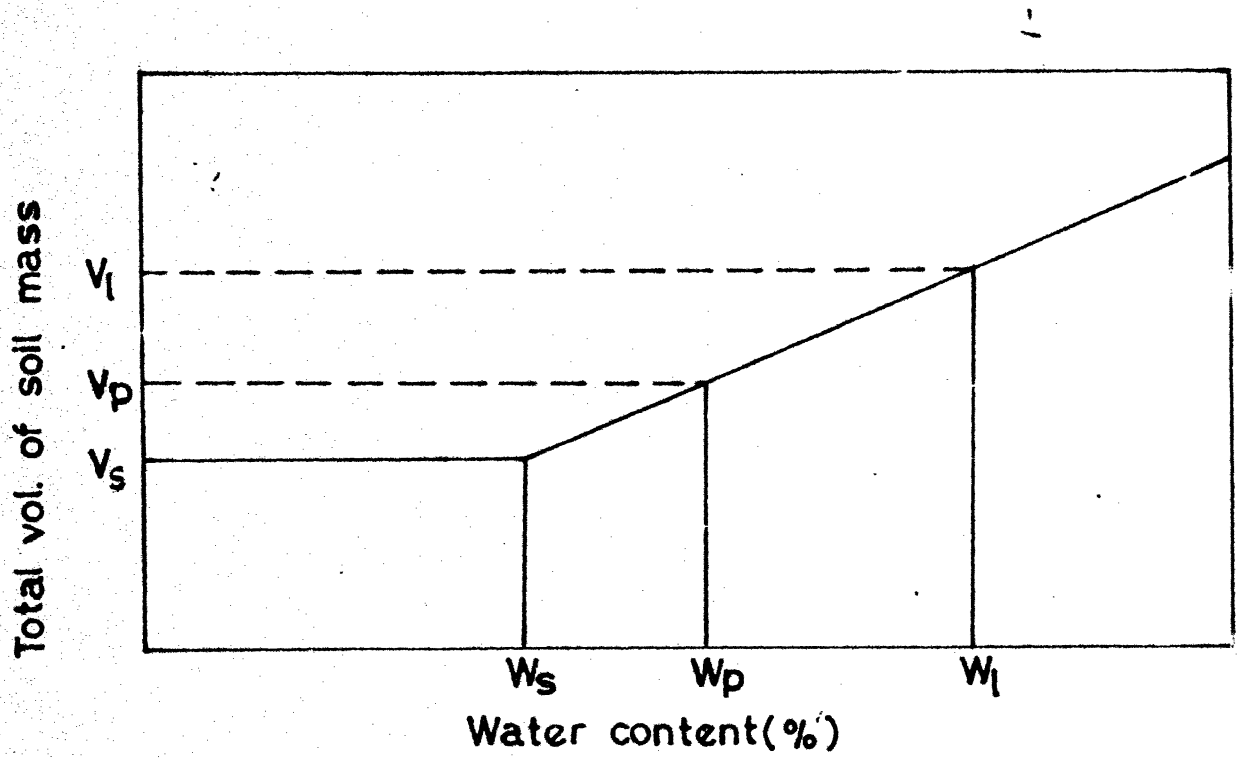

Fig.2.1 Consistency limits

CHAPTER 3

MATERIALS AND EXPERIMENTAL

3.1 Rice Husk Ash:

Two different types of Rice Husk Ash were used for characterization and development of field tests.

A. The ash samples were prepared by first combusting small heaps of rice husk at a nominal temperature of 350°C in an electric muffle furnace, followed by subjecting the resultant ash to 450, 600, 800, 1000, 1200 and 1400°C in sillimanite crucibles for 12 hours. A separate thermocouple was provided to observe the temperature of the burning heap of husk, while the furnace temperature was maintained at 350°C.

B. A number of rice husk ash samples used in liquid limit tests were prepared by burning rice husk in the laboratory in a tube in basket (TIB) furnace designed by Kapur.[1] The overall burning of husk in the burner is due by two combustion processes that occur simultaneously, (i) combustion of volatile matter at the mouth of the burner tube and (ii) direct burning of remaining wood tar and fixed carbon in the husk bed. The ash obtained from the furnace was almost completely free of carbon.

3.2 Null Pychnometer and Density Measurements:

Null pychnometer is used to measure the volume of solid or powder accurately. This technique uses the principle of pressure differences in the sample holder with and without the solid under examination. Figure 3.1 gives the working diagram of Null pychnometer. The shaded area is considered as the sample holder.

When the syringe 'S' is depressed the pressure in the cell holder increases and the differential gauge 'G', indicates a pressure difference. Gas is allowed to flow under pressure through needle valves 'N_1', 'D_2' and 'T_2' to pressurize 'G_2' and rebalance the null gauge when 'G_1' is exactly nulled the reading on 'G_2' is taken. This procedure is performed two times once with the sample cell empty and again with powder in the cell. From the readings taken on 'G_2' the powder volume is calculated using

$$V_p = V_c (1 - P_2/P_2')$$

where P_2 is reading on Gauge 'G_2' when 'G_1' is nullified with no powder in the sample cell,

P_2' is reading on Gauge G_2 when Gauge G_1 is nullified with powder in the sample cell,

V_p is volume of powder (cm^3)

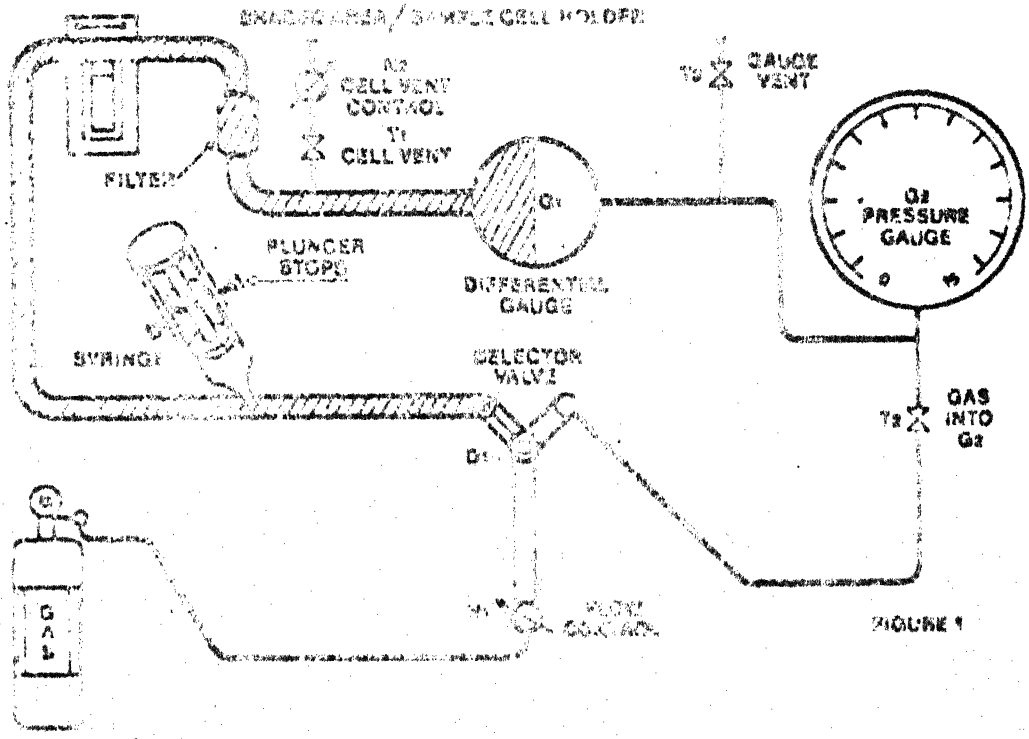

Fig. 3.1. NULL PYCNOMETER.

V_c is volume of sample cell Holder (cm^3),

154.88 cm^3 for large sample cell holder

30.92 cm^3 for small sample cell holder

Rice Husk Ash samples ground and sieved through 270-mesh screen were used for the density measurements.

3.3 X-Ray Diffraction:

X-ray diffractions were conducted on XRD-5 machine. The machine/test parameters, kept constant in all tests, were as follows.

Target	Copper
Radiation (°A)	K (1.5405)
Filter	Nickel
Target voltage (KV)	30
Target current (mA)	15
Slit width	3°
Scanning range	10-60°
Counts per second	2

3.4 Electron Microscopy

Scanning electron microscopy of heat treated rice husk ash was carried out using ISI 60 Scanning Electron Microscope.

The samples for the above analysis were prepared by first suspending rice husk ash in acetone and taking the suspension on Aluminium Substrates (sample holder). The substrates were

subjected to gold coating by Evaporation method. The sample holder was mounted in its position in the electron microscope and photographs were taken using different magnifications. The operating parameters of EM were :

Voltage 30 kV

Secondary Electron mode

3.5 BET Test:

Since the facilities for measuring the physical adsorption of gas on powder sufface were not available, BET tests were got done on Orr. Surface Area Analyzer Model 2100D at the Univ. of California, Berkely.

3.6 Mercury Penetration Porosimetry:

The Hg porosimeter, Micrometrics Model 900/910 series, which was employed for the pore structure study did not have any provision for the analysis of powder samples. At first the powders of rice husk ash were made in the form of pellets under different pressures in a laboratory caver hydraulic press. In order to impart sufficient strength to pellets, it was necessary to use 5% polyvinyl alcohol as binder.

Figure 3.2 . shows that the Hg - porosimetry results were highly dependent on the pressure employed in packing the pellets. This was due to breaking up of fragile pores in ash particles during pressing as well as formation of new pores by interlocking of particles. This approach was therefore abondoned.

Next, a simple technique was devised to study the powder samples directly. Steel holder of about 2.2 cm in dia and about 1 cm in height were filled completely with rice husk ash by gentle tapping. The mouth of the holder was covered with a circular disc net from a 300- mesh stainless steel screen. Since the wire mesh was fine, a threshold pressure was needed for mercury to penetrate into the sample holder through the wire mesh. The break through pressure was determined by running a blank run with empty sample steel holder and the regular runs were corrected accordingly.

The mercury penetration technique requires a mean for generating pressure and a mean for determining how much mercury the application of a given pressure has forced into the pores or void spaces of the material being tested. The general arrangements of micrometrics Hg-porosimeter is shown in fig. 3.3.

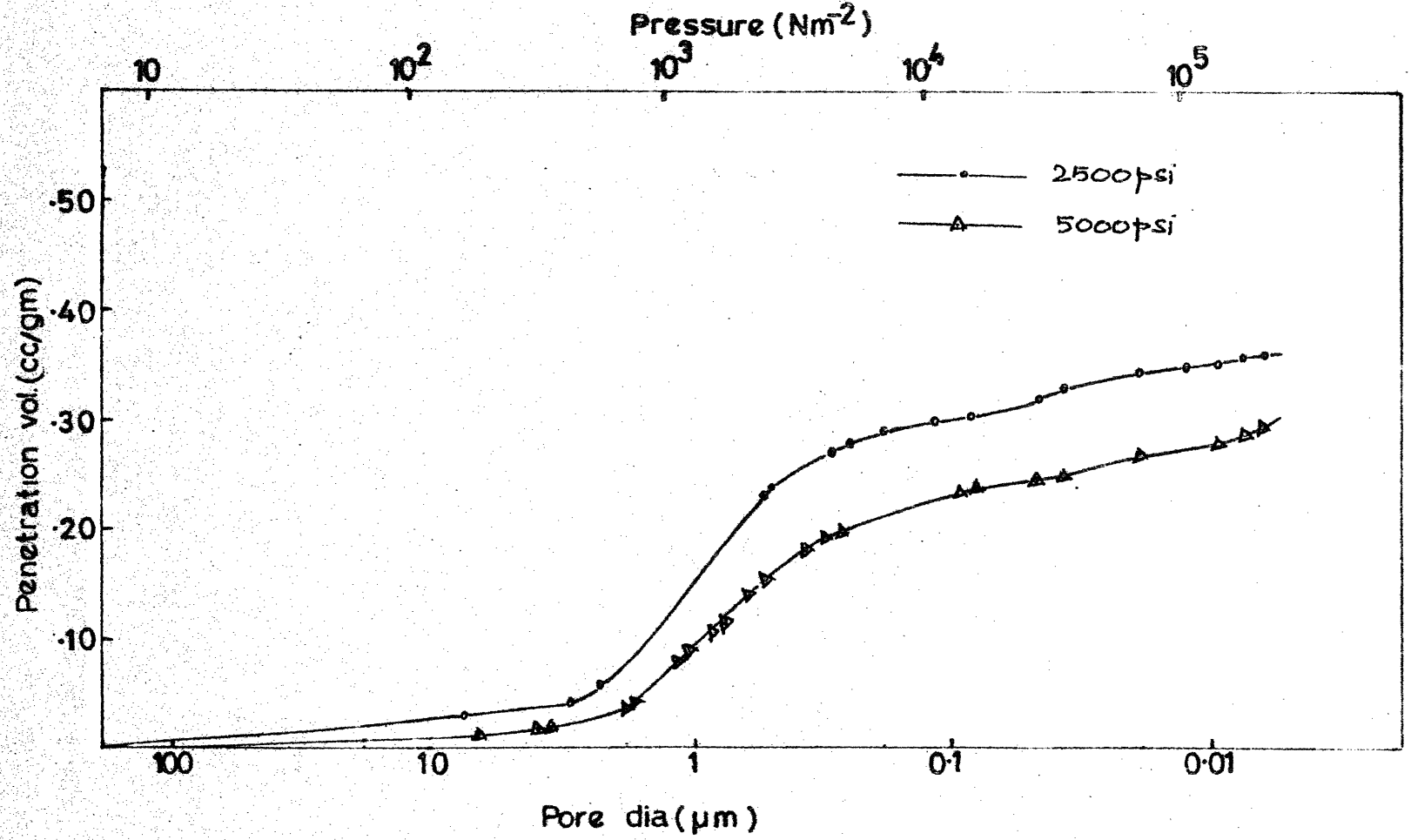

Fig. 3.2 Effect of pressure on the pore volume of rice husk ash

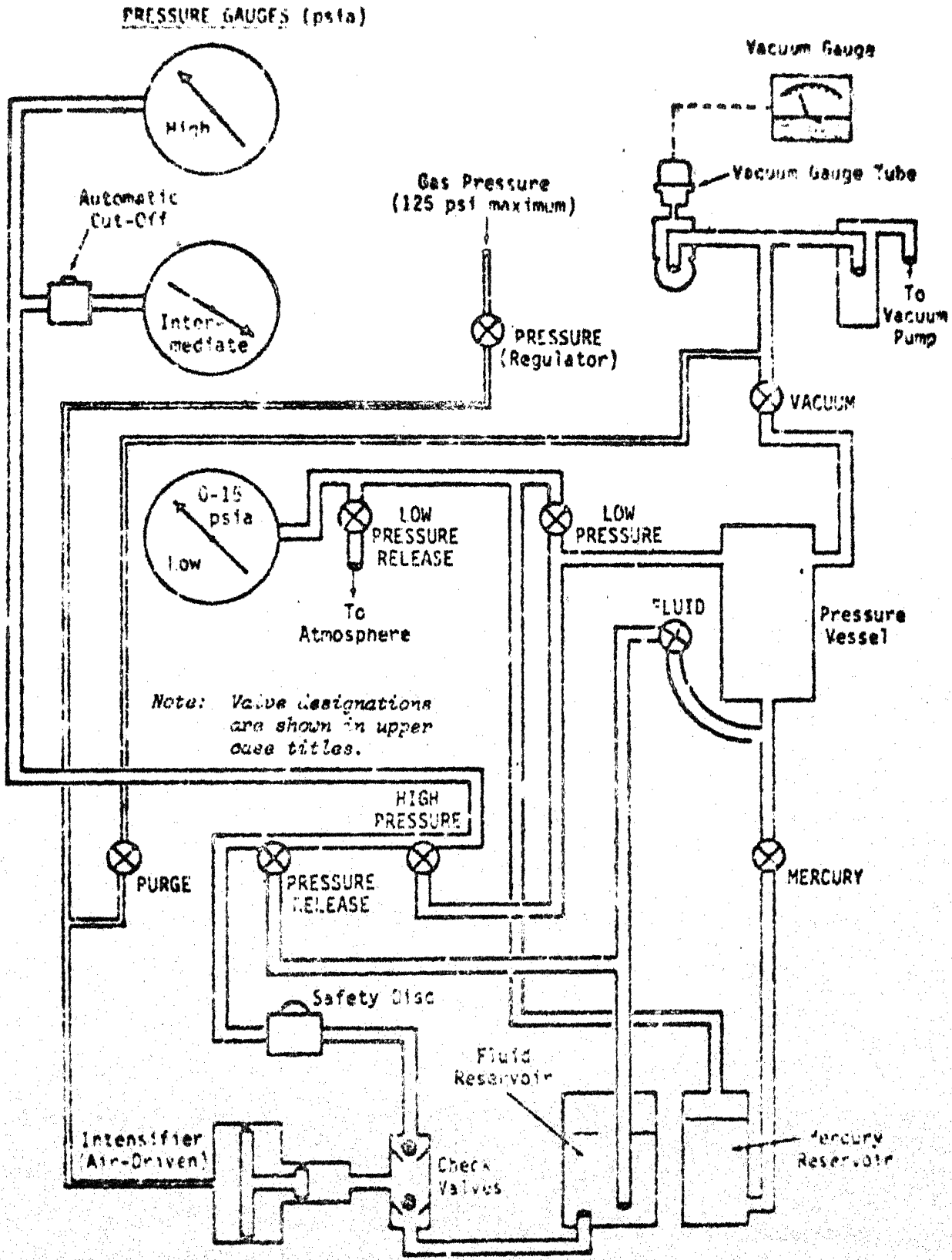

FIGURE 3.3. SCHEMATIC DIAGRAM OF POROSIMETER

The top of the pressure vessel (heavy walled steel vessel) can be removed and remounted in position. The top carries a fixed electrical contact that dips into the cup on the top of the glass sample cell (fig. 3.4). It also carries a movable contact that follows the mercury down the bore tube of the sample cell as pressure forces the mercury in the pores within and void spaces about the test material. The extent of this movement is indicated electrically. The sample is placed in the sample cell and the holder is then put into the pressure chamber. The first operational step is to remove the gas and vapor from the sample space and from the pressure chamber once the pressure chamber is evacuated, mercury is let into the pressure chamber indicating the sample holder filling it with mercury and filling the cup or tube at the top of the sample holder. Sufficient air pressure is admitted into the chamber to permit mercury, except for that caught in the sample cell, to drain out. The sample is completely surrounded by mercury and as pressure is applied the mercury penetrates into the sample. The changes in the mercury level is indicated automatically on a counter as the movable contact follows the mercury. The readings of mercury entered as function of pressure were recorded. The tabulated data is given in Appendix.

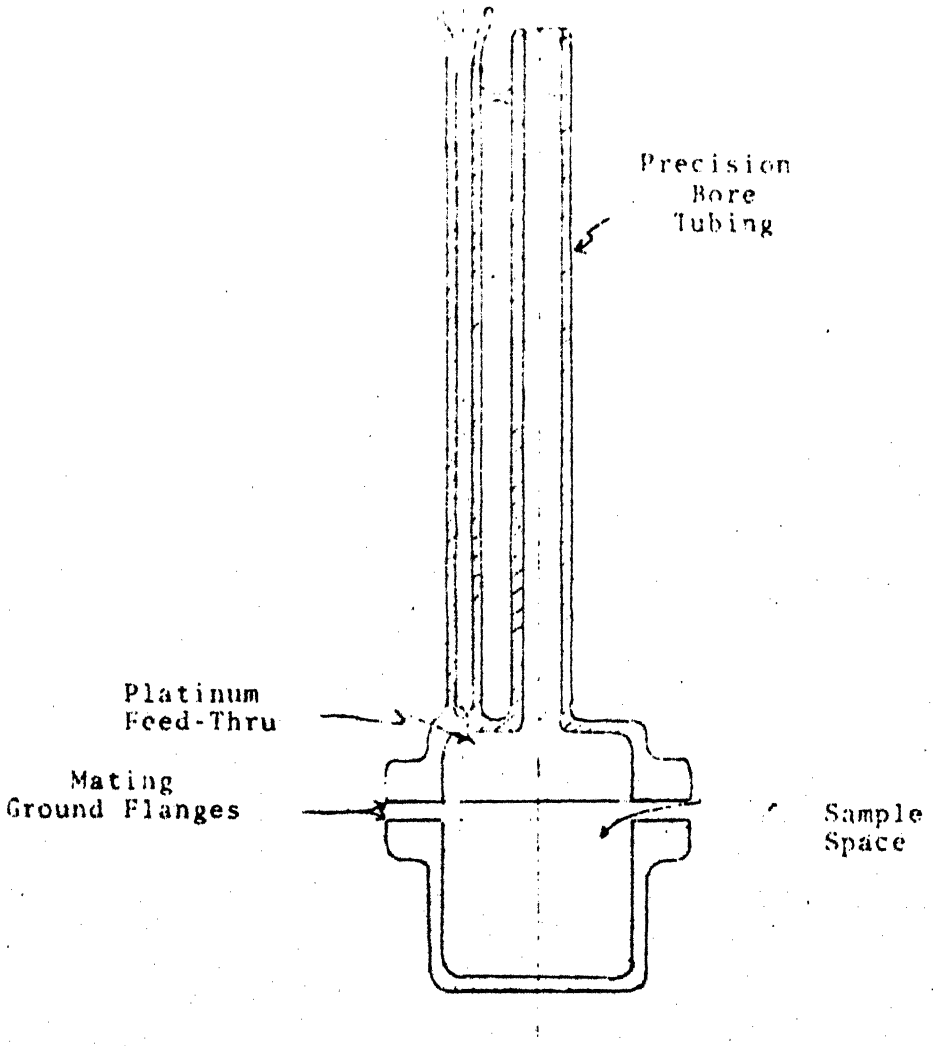

Figure 3.4. Large-Piece Sample Cell

3.7 Liquid Limit Tests :

Liquid (Water or Kerosene) was taken in a burette and allowed to wet a known quantity of rice husk ash in a dish with vigorous mixing with a spatula. First the ash pores were filled then semidry crumbs of ash particles were formed and finally with addition of more liquid, the whole material became a single coherent wet mass, with a thin dark colour rim of liquid all around it. This transition from crumbs to coherent mass was quite sharp and reproducible after a little bit of practice. The amount of liquid used was recorded. The data is given in Appendix.

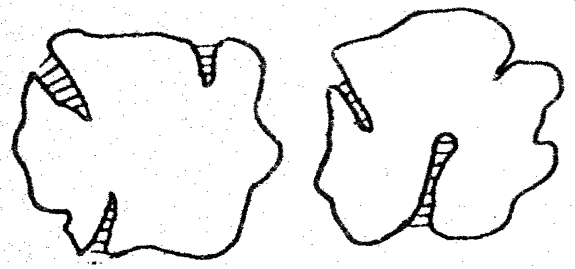

Semidry powder

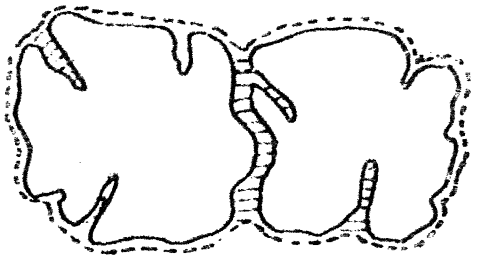

Loose crumbs of powder

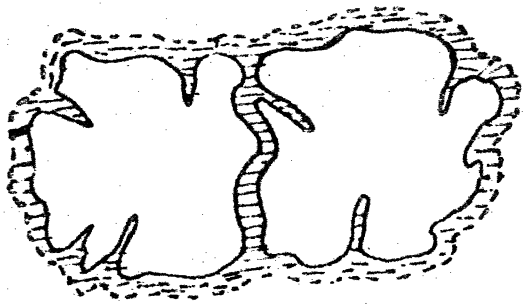

Liquid limit

Powder covered with liquid film

Fig. 3.5

CHAPTER 4

RESULTS AND DISCUSSION

4.1 Firing of Rice Husk:

The typical temperature profiles of the furnace and that of a heap of husk of about 75 mm base diameter and 80 mm high are shown in fig. 4.1 when the temperature controller was fixed at 350°C. In course of its combustion the temperature of the husk bed shot to 600°C eventhough the temperature of the furnace was maintained at 350°C. Under the chosen experimental conditions this was the minimum temperature at which husk could be burnt to produce essentially carbon free ash. The resultant ash was dirty brown in colour. Other investigators have not made any distinction between the two temperature profiles, i.e. in the furnace and the heap. Therefore their reported values of temperature of combustion are suspect.

On heat treating the burnt husk from 600 to 1200°C the colour of the ash changed from light brown to white as shown in Table 4.1. This could be due to the oxidation state of the multivalent cation impurities, specially iron. The ash produced at 1400°C showed slight brownish colour because of the reaction of rice husk ash with the sillimanite crucible.

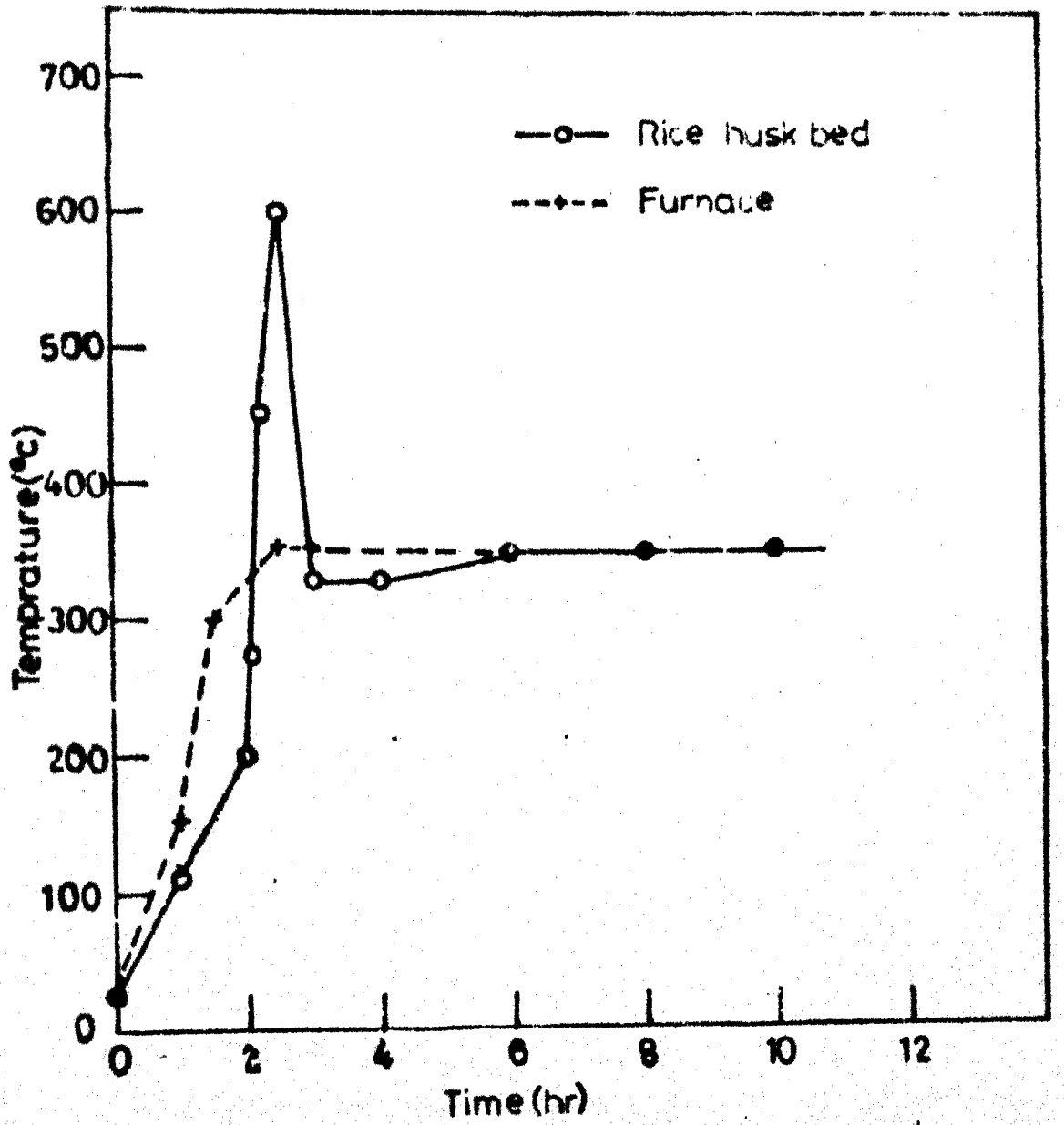

Fig 4.1 – Temperature profiles of furnace and husk bed

TABLE 4.1

Colour of Rice Husk ash at Different temperatures of heat treatment

Temperature °C	Colour
350	light dirty brown
450	dirty brown
600	light brown
800	red pink
1000	light pink
1200	pure white
1400	light yellow

4.2 Bulk and Apparent True Densities:

The variations of tapped bulk and apparent true densities of rice husk ash burnt at different temperatures are shown in figure 4.2. In general, both densities show an increasing trend with increase in temperature on account of reduction in the pore volume of ash by sintering and the formation of crystalline phases of silica which are known to be denser than the original amorphous silica phase formed at the lower temperature. The bulk density results are somewhat erratic. The packing density depends on the size distribution of the particles also, and the extremely friable ash particles

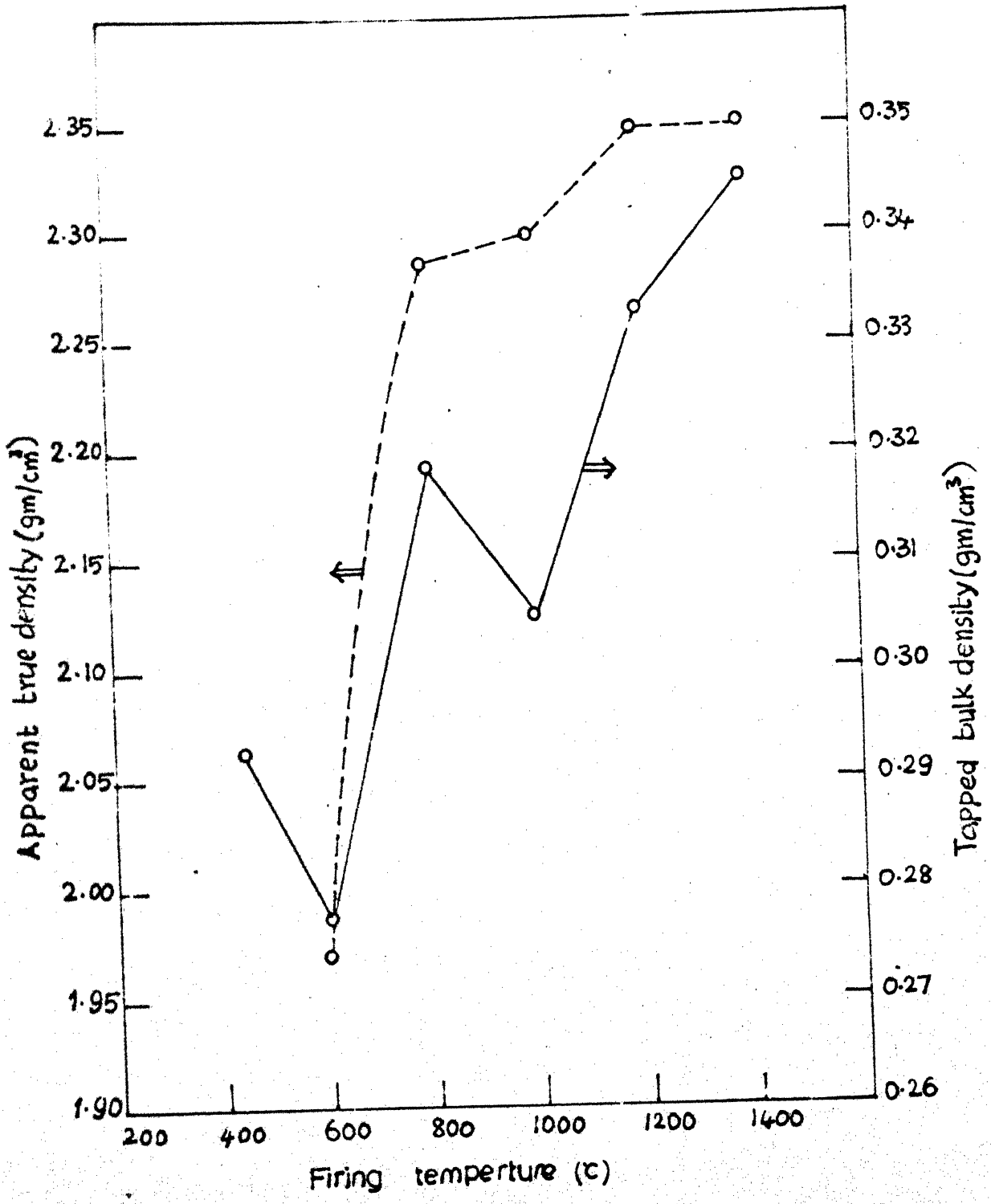

Fig 4.2 Tapped bulk density and apparent true density of rice husk burnt at different temperatures

had undergone size degradation to different extent, depending on the degree of handling of ash samples. The specific gravity of common room temperature stable silica phase are [19].

β - quartz	2.65
γ - tridymite	2.26-2.28
β - crystobalite	2.31-2.32
silica glass	2.2

The true density results in fig. 4.2 indicate that phase transformation or devitrification of silica occurs continuously and rapidly over the temperature range 600 to 1000°C, and that final principal phase formed is crystobalite; results which were verified by X-ray Analysis.

4.3 X-ray Analysis:

Figures 4.3 and 4.4 show the x-ray diffraction patterns of rice husk heat treated at various temperatures and of six randomly chosen ash samples from a TIB burner.

It will be observed that the 450°C fired rice husk ash sample is completely non-crystalline. Crystalline quartz starts forming only at around 550°C, but disappears in 1000°C and higher samples. These results are in conflict with those of Hanafi et al[9] who reported no indication of quartz peak at any temperature range, but are in agreement with the work of Vijaya Bhaskar[1].

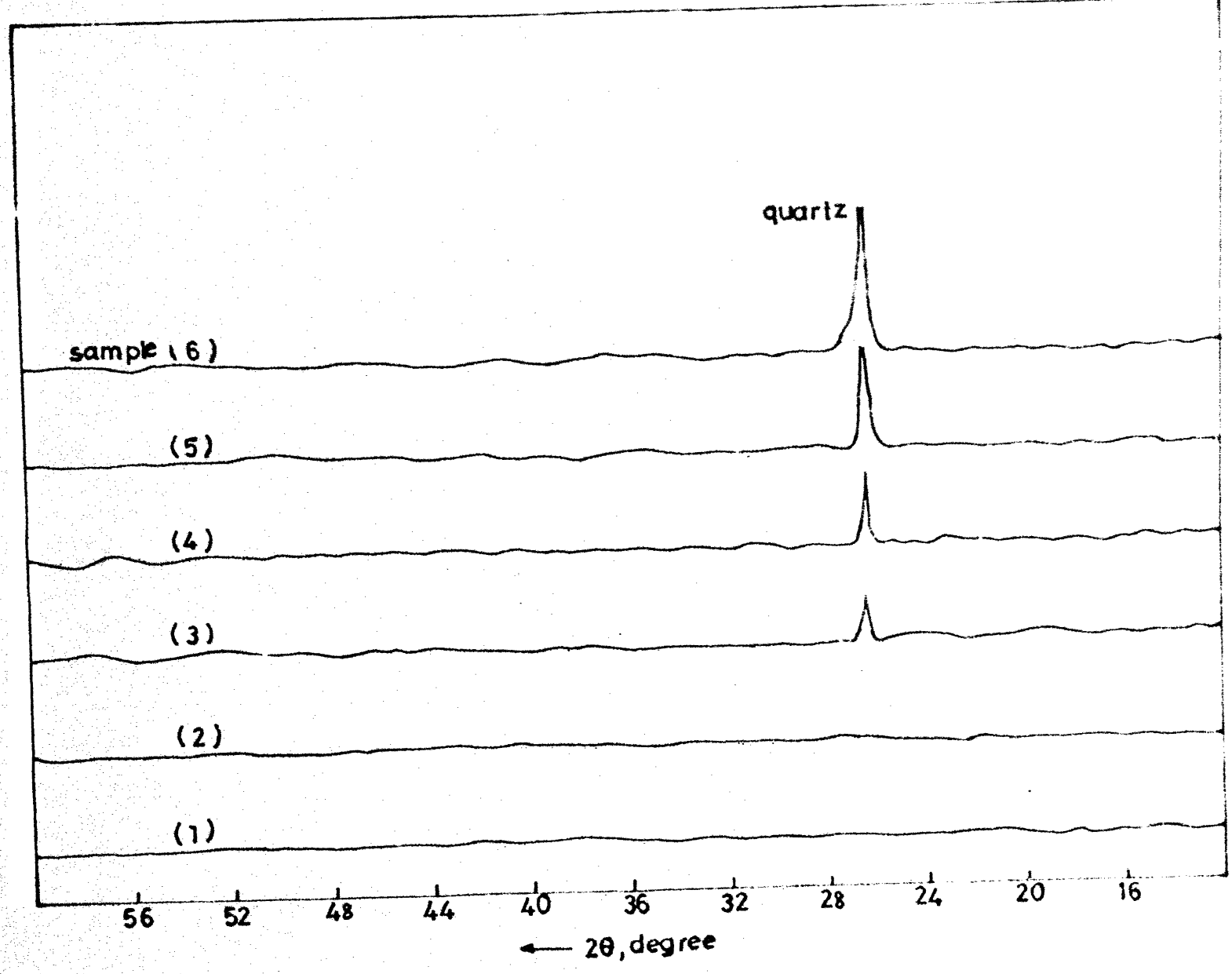

Fig 4.4 X ray data on fired T13 ash samples

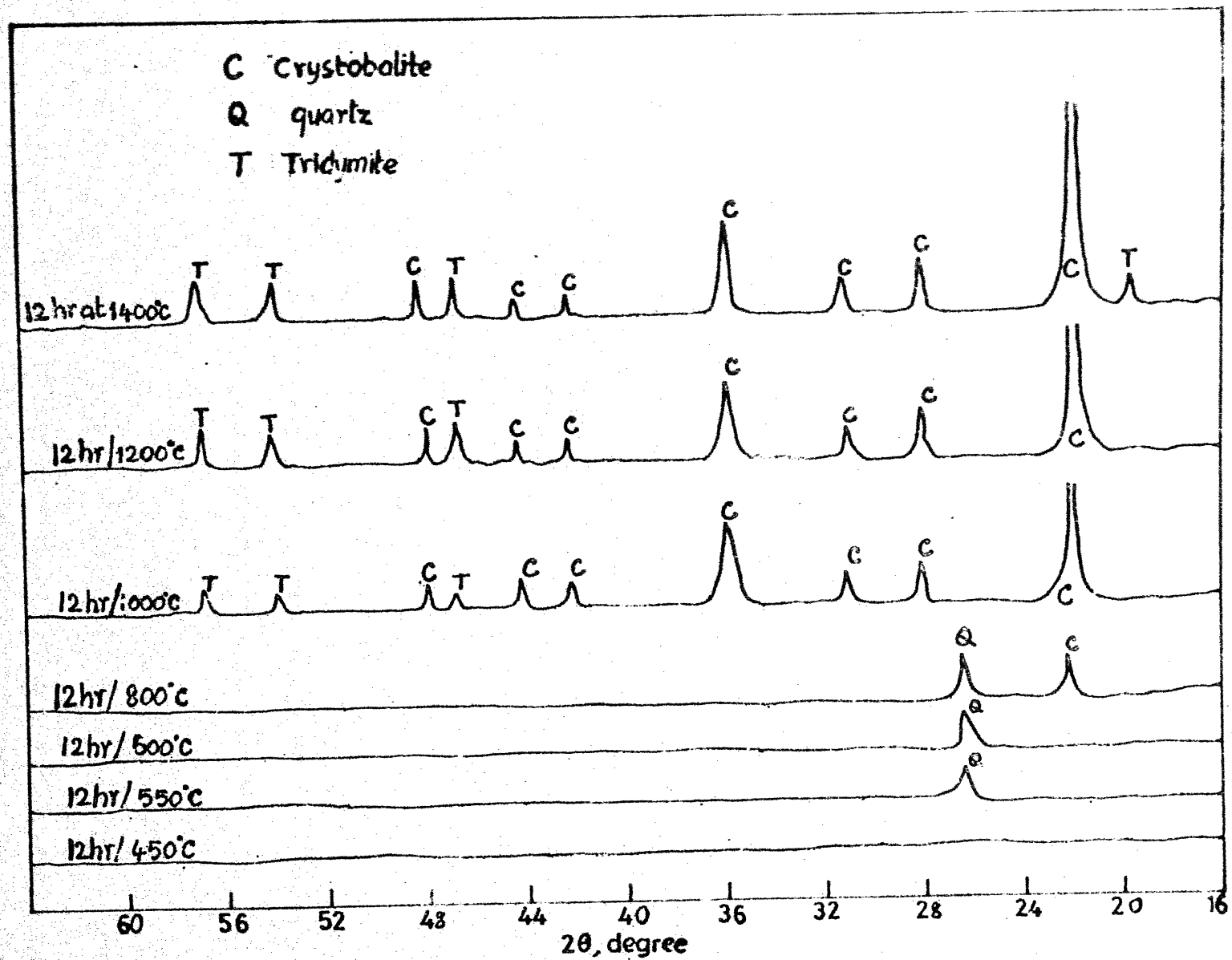

Fig. 4.3 X-ray data on heat treated rice husk ash at different temperatures

The crystalline crystobalite phase first appears at 800°C without any change in the amount of quartz. Between 800° and 1000°C massive transformation to crystobalite occurs. Besides this phase, tridymite phase also starts to form at 1000°C, the amount increases somewhat between 1000 and 1200°C. Between 1200 and 1400°C, both crystobalite and tridymite phases seem to coexist without much alteration in their relative proportions.

TIB ash samples were classified according to their colour varying from partially burnt husk ash with some carbon in it (black in colour) to completely burnt white ash.

X-ray Analysis of six different coloured husk ash samples namely dark grey, light grey, light brown, brownish red, light pink, pink white and white and marked as 1, 2, 3, 4, 5 and 6 was done. The samples (1) dark grey and (2) light grey do not show any sign for crystallinity, and only amorphous silica exists in the above two cases. Quartz is detectable in the remaining samples and the intensity of its peak increases gradually as colour changes from light brown to white as shown in fig. 4.4. It is concluded that TIB ash is in general amorphous and due to its high reactivity suitable for making cements. Colour is related indirectly to the amount of heat treatment of ash and this is reflected in the appearance and amount of quartz.

4.4 Surface Area by BET

In figure 4.5 the BET specific surface area of rice husk ash is plotted as a function of temperature. The surface area increases slightly at first and then decreases drastically as the firing temperature increases. The magnitude of the specific surface area of these samples indicates that the rice husk ash possesses an enormous internal surface area and the porosity decreases with temperature. The slight increase in specific surface area initially is due to burning off of residual carbon and opening up of additional pores. The steep fall in surface area thereafter is caused by sintering and closing up of pores accompanied by phase transformation from amorphous to fully crystalline states of silica.

4.5 Mercury Porosimetry :

4.5.1 Pore Volume and Porosity:

The mercury penetration curves (volume versus pressure/pore dia) of rice husk ash treated at 600, 800, 1000 and 1200°C are shown in fig. 4.6. These graphs were drawn after making correction for the pressure to penetrate the wire mesh and the volume of mercury that entered into the sample holder and surrounded the powder particles through the wire mesh. Cumulative pore volume greater vs pore size for various samples is shown in figure 4.7. It is quite clear from figures 4.6 and 4.7 that the apparent porosity decreases substantially when the firing temperature is increased. The porosity 0.353 cm^3/gm at 600°C is decreased to approximately one sixth, 0.065 cm^3/gm at 1200°C. The decrease in porosity is due to sintering at high temperatures leading to closing of pores and

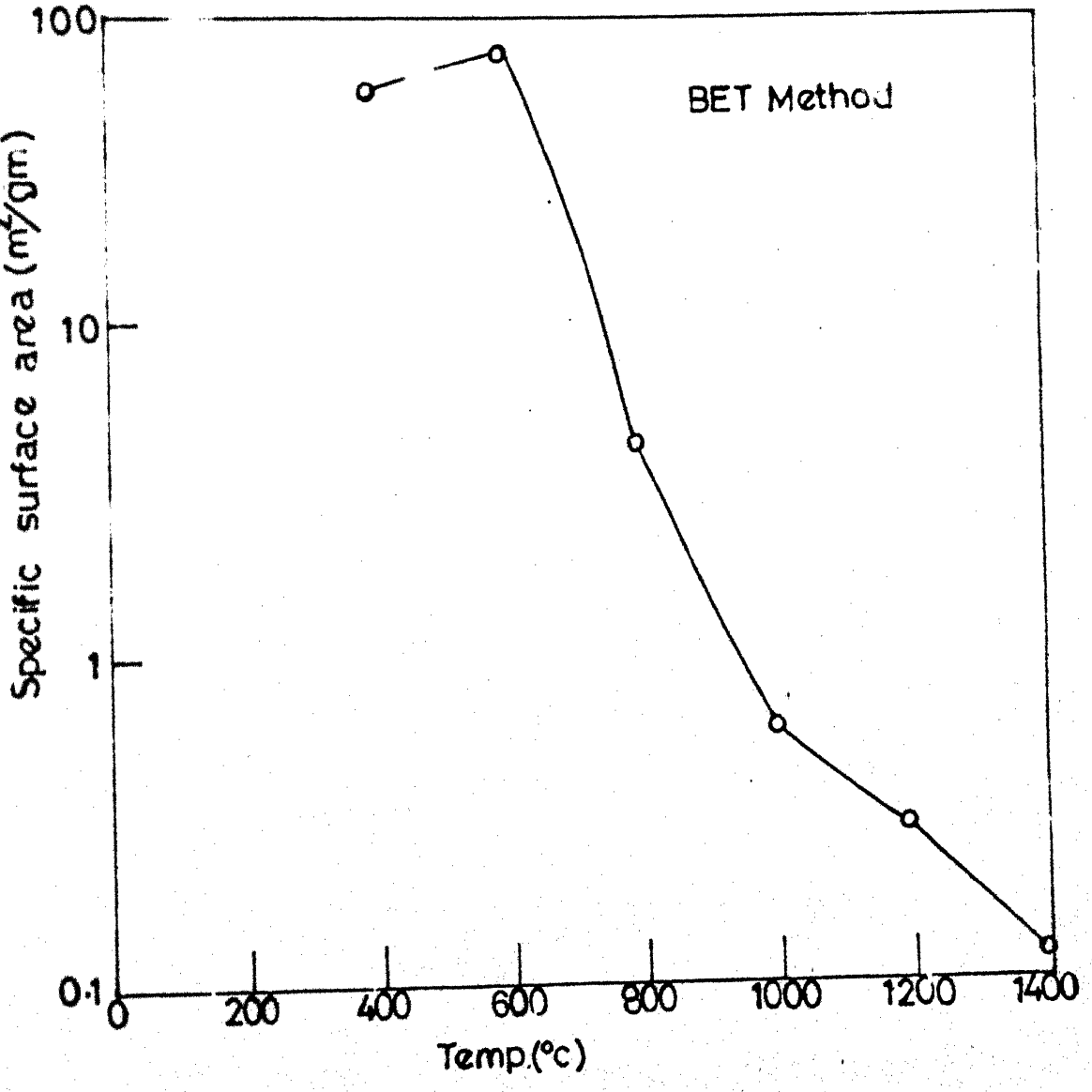

Fig.45 Sp. surface area of the rice husk ash silica with temp. of thermal treatment

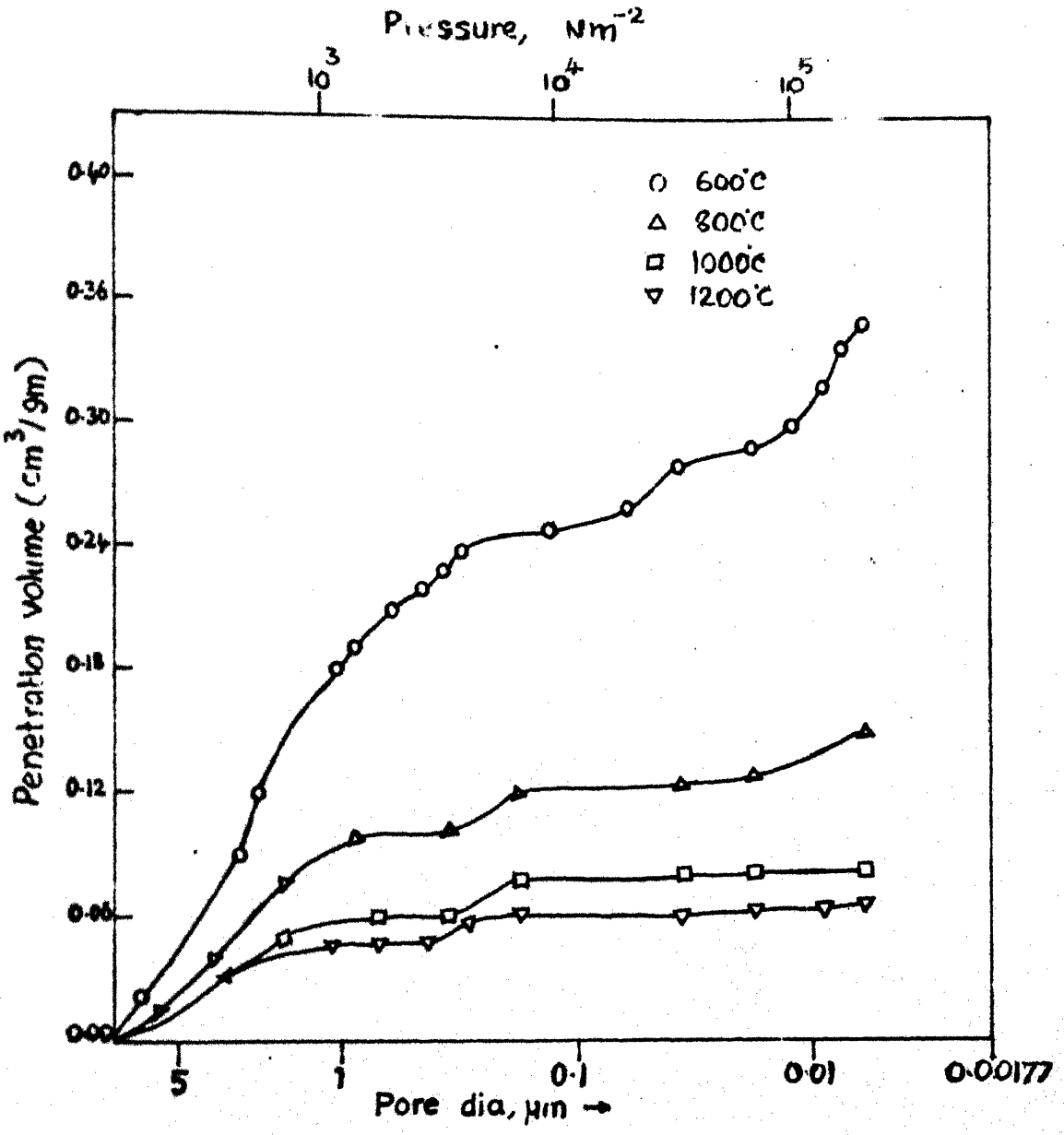

Fig.4.6. mercury penetration curves of fired rice husk ash

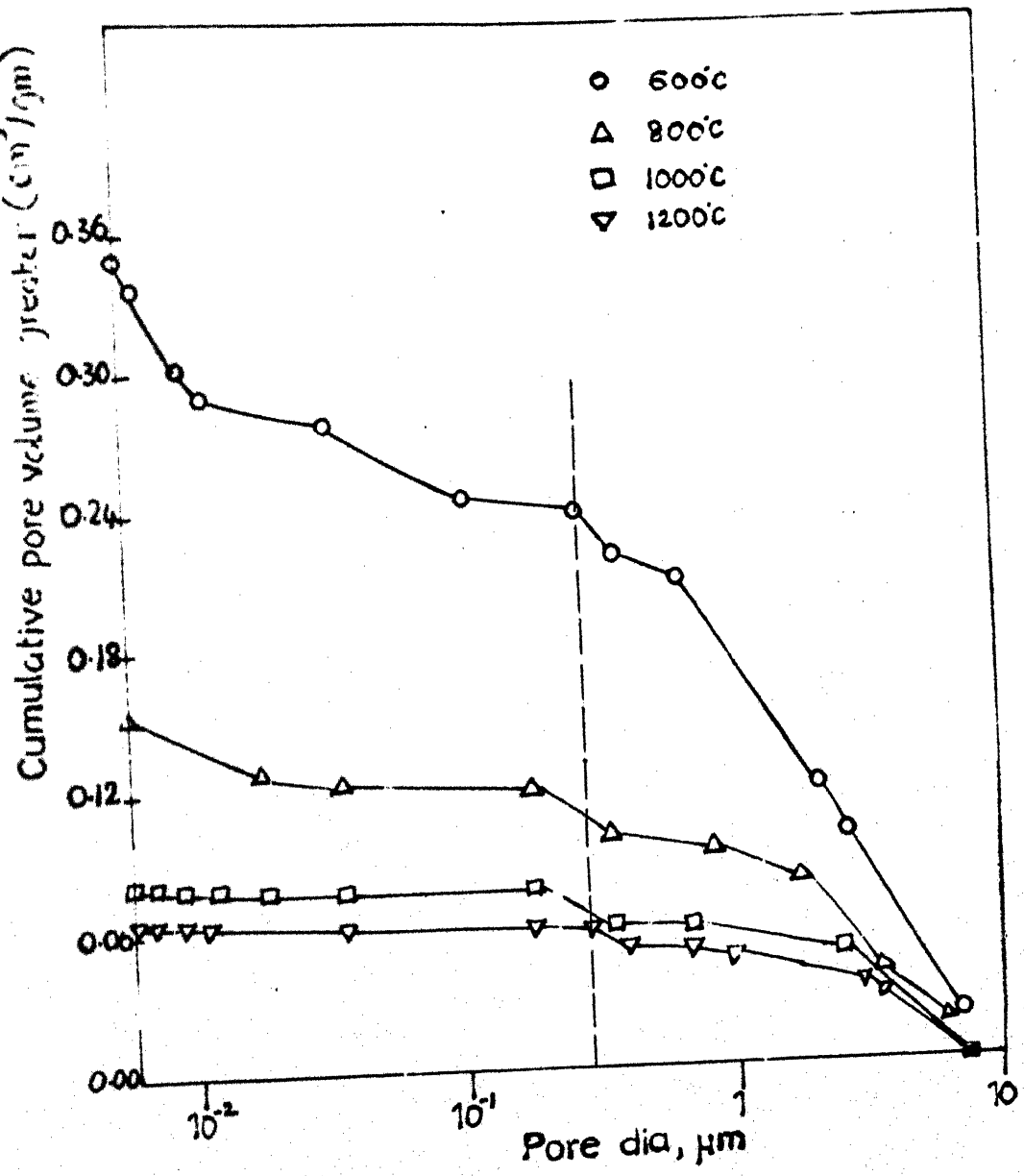

Fig.47 Cumulative pore vol. of fired rice husk ash samples

It is clearly observed from these figures that there exist two types of pores. A vertical dotted line drawn in figure 4.7 at D=300 nm separates each cure into two sections. The pores greater than 300 nm are macropores and are observed in all the samples. The 600 and 800°C ash samples contain both macro and mesopores (> 2 nm) but the overall porosity is mostly due to macropores. The curves of 1000 and 1200°C samples flatten at high pressures, which indicates the presence of negligible amount of open and accessible to mercury macropores. The upward trend of curves for 600 and 800°C samples at the maximum Hg pressure used in figure 4.6 indicates that all the pores have not been filled with Hg due to limitation of the apparatus.

The relative apparent porosity values decrease with increase of firing temperature as shown by the cumulative pore volume distribution (figure 4.7) at any particular pore dia. Figure 4.8 shows graphs of macro-, meso- and total porosity as a function of firing temperature of ash samples. The total porosity varies from 41% for 600°C ash to 13.25% for 1200°C ash. Over 75% of porosity is in macroporous range in 600°C and 800°C samples while it is 90% in the case of 1000°C and 1200°C samples.

4.5.2 Pore Size Distribution :

The pore size distributions of heat treated rice husk ash samples were calculated and are presented in fig. 4.9. All the curves show similar effects, i.e. a bimodal distribution with one peak in the macroporous range of 100 nm to 600 nm

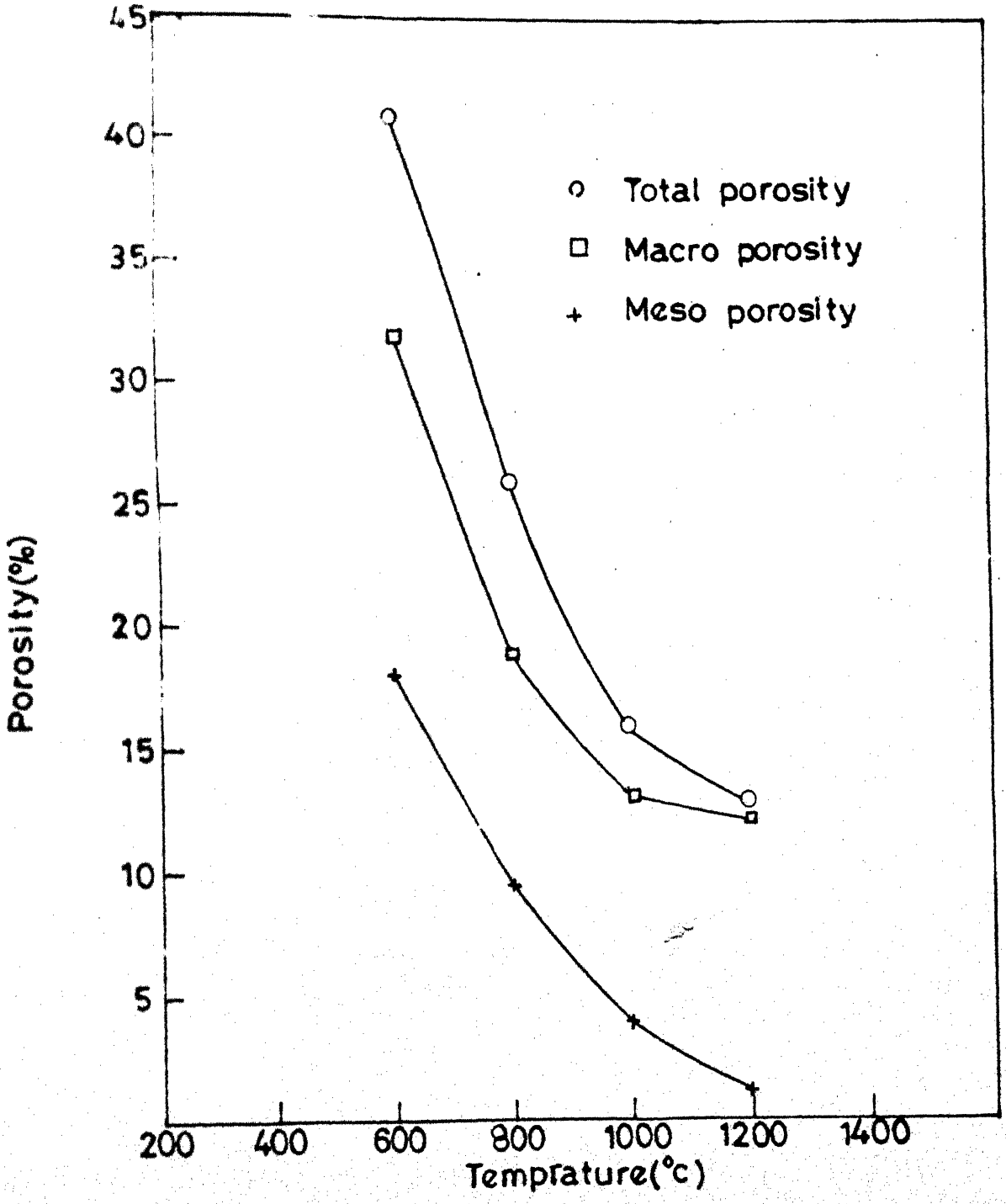

Fig.48 Porosity of rice husk ash as a fuction of firing temprature

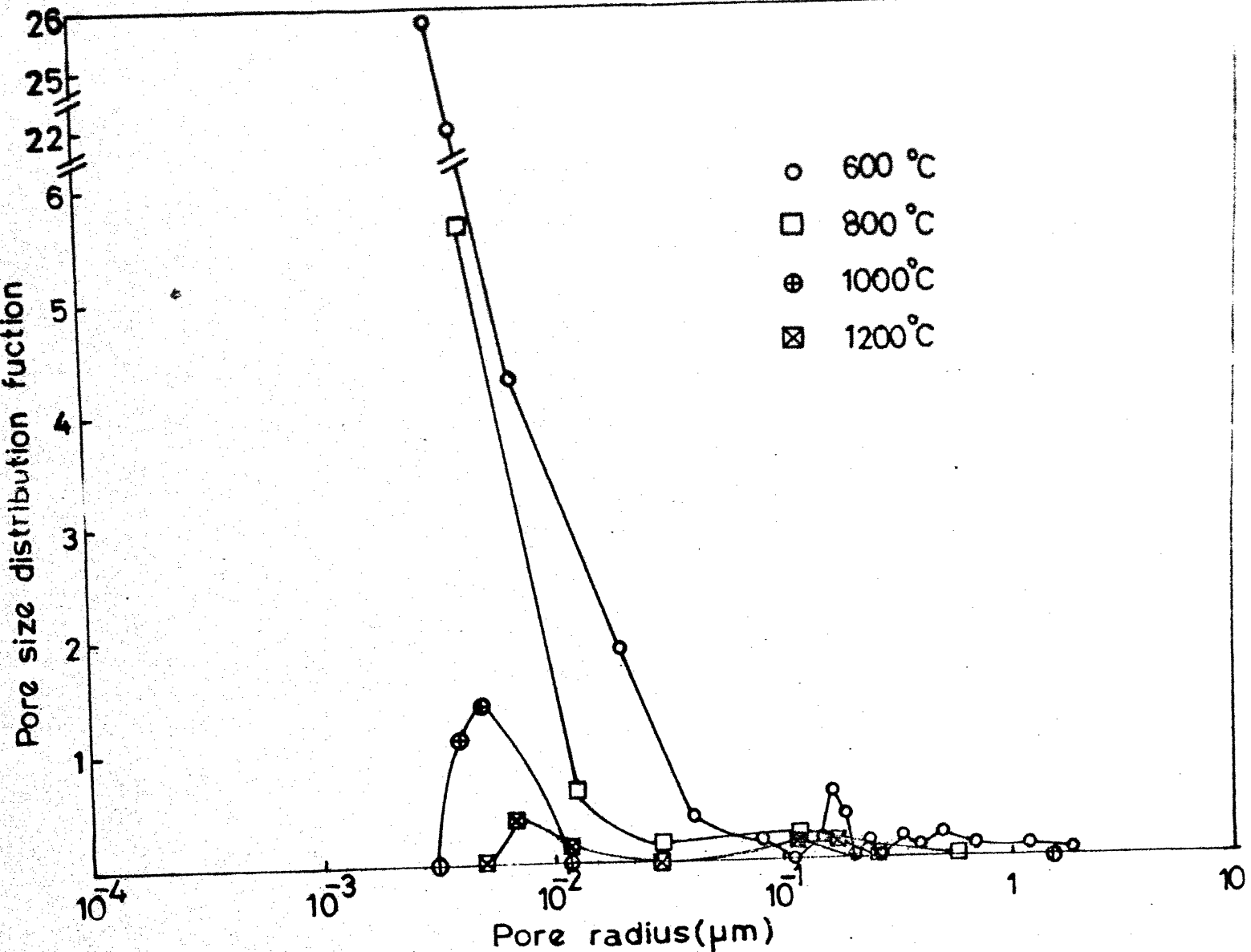

Fig.4.9 Pore size distributions of various rice husk samples

and the other in the mesoporous range of 3 nm to 8 nm. In the meso - range the two peaks of 1000 and 1200°C ash are at 5nm and 7 nm respectively and are well defined. Sharp increase in pore volume is noted in the other two samples, but the exact location of the peak could not be determined. The mode of pore volume frequency function is shifted regularly to higher pore size with increase in firing temperature. The distribution of pores became more uniform, narrower in spread and shifted towards larger size range as the firing temperature is increased.

4.5.3 Specific Surface Area:

The specific surface areas shown in fig. 4.10 were calculated using Rootare and Penzlow formula presented in Chapter 3. The highest observed specific surface area is 38.12 m^2/g for 600°C which drops rather abruptly to 0.97 m^2/g for 1200°C sample. A similar trend was observed in BET surface area in Fig.4.5 but the surface area values do not match for a number of reasons.

i) The maximum pressure in Hg porosimetry was 207×10^3 KNm^{-2} reaching a minimum pore diameter of 6 nm. Hence a part of mesoporosity and whole of microporosity was not accessible to Hg.

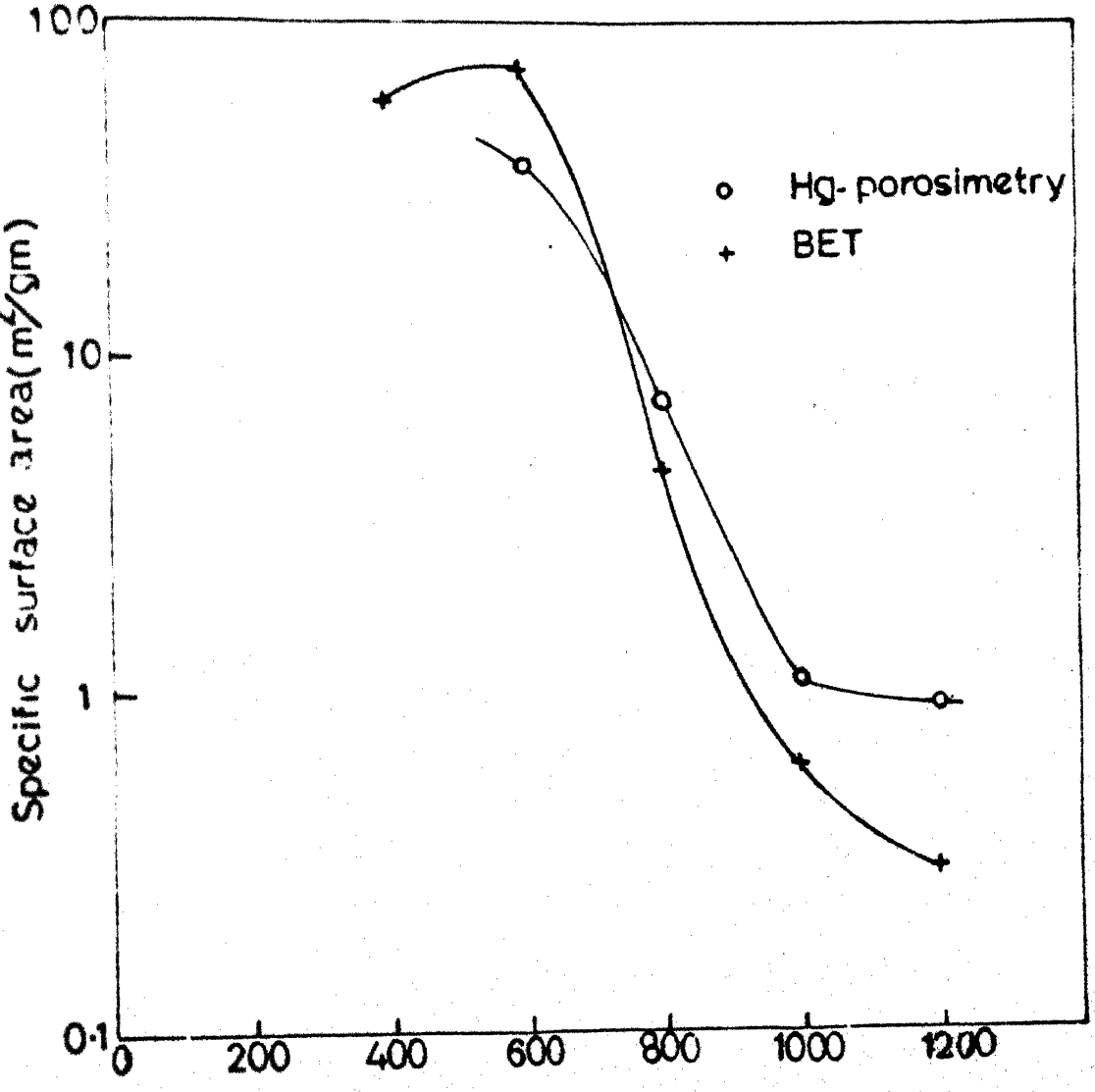

Fig. 4.10 Sp. surface area of the rice husk ash silica with temp. of thermal treatment

ii) The thin walled and fragile structure of porous ash could have collapsed somewhat under high Hg - pressures leading to both closing up of pores and opening up of closed pores by fissure and fracture.

iii) The correct contact angle value for Hg with ash material is not known.

Further it is also reported in the literature[22] that he calculated surface area by means of the expression

$= \frac{pdv}{\gamma \cos\theta}$ amounts in most instances to only 60% of the alue derived from gas adsorption.

.6 Pore Structure by SEM:

Scanning electron microscopy photographs are shown for relatively low temperature fired husk ash at 600°C and a high emperature fired ash at 1200°C taken at different magnifica-ions. The pore structure of the ash samples are clearly seen. s the temperature of firing increases from 600°C to 1200°C here is an observed difference in their pore structure. ores of smaller size disappeared and the large open pores get losed in 1200°C ash sample. This is also revealed by the ore size distribution, density and pore volume or porosity easurements.

4.7 Liquid Limit:

The results of the liquid limit tests, developed for field tests of rice husk ash are presented in fig. 4.11 which shows that water and kerosene give essentially similar results and the liquid limit trend is remarkably consistent with x-ray, porosity, surface area trends described before, namely, there is a marked drop in the liquid limit between 600° and 1000°C. Figure 4.12 shows the effect of particle size of ash on this test. Highest liquid limit is obtained with coarsest sample and kerosence. In finer samples the pore structure is broken down and lower liquid limit value results. It is therefore desirable to employ coarse samples with kerosene for greater sensitivity of the test. Fig. 4.13 shows liquid limit results for TIB ash samples employed for x-ray analysis (fig. 4.4). The samples are well differentiated and the results are again consistent with the amount of crystalline phase detected by x-ray. It seems then that this inexpensive and simple test might be useful for field evaluation of rice husk ash reactivity, specially for comparative and routine quality control.

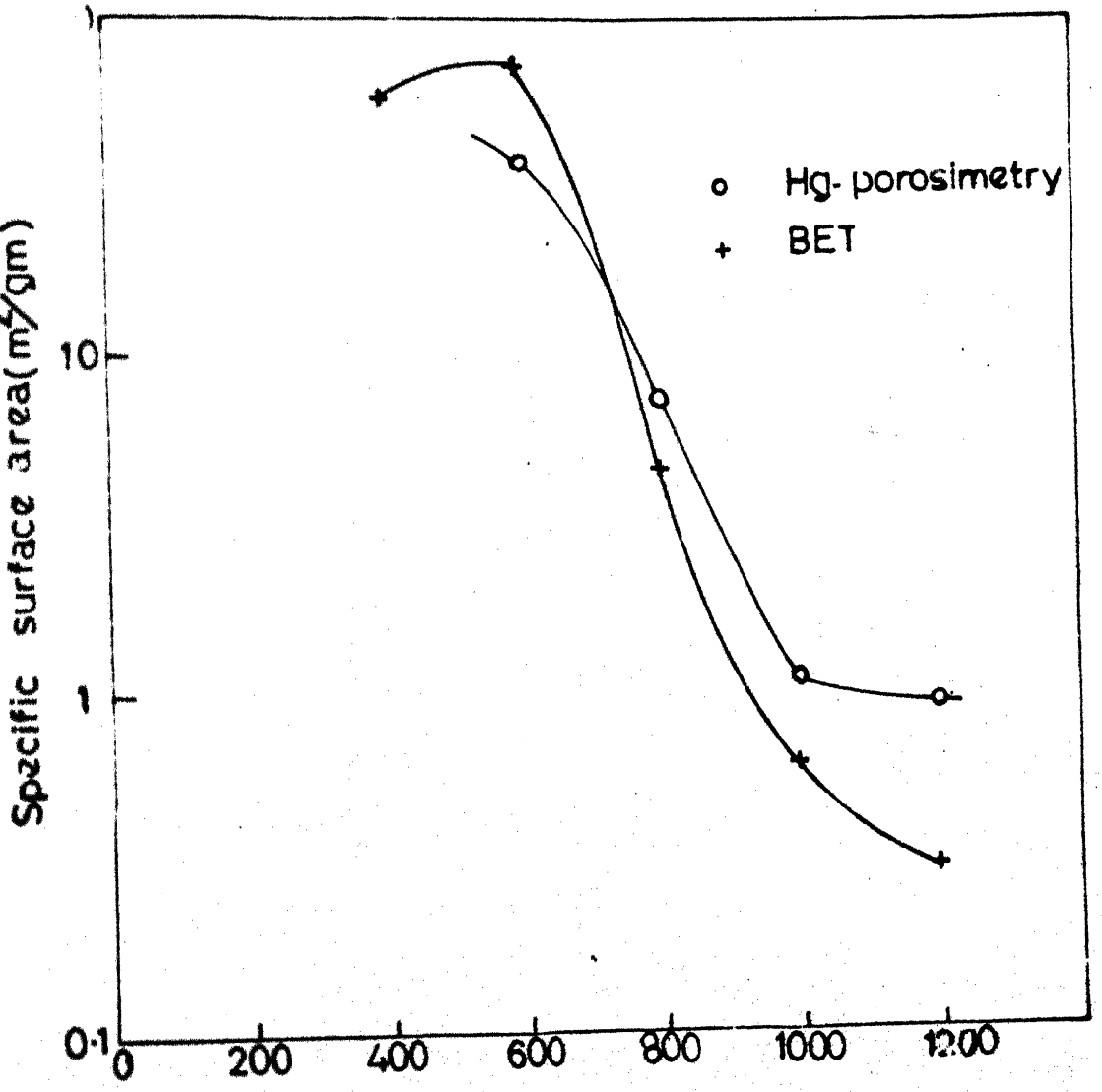

Fig. 4.10 Sp. surface area of the rice husk ash silica with temp. of thermal treatment

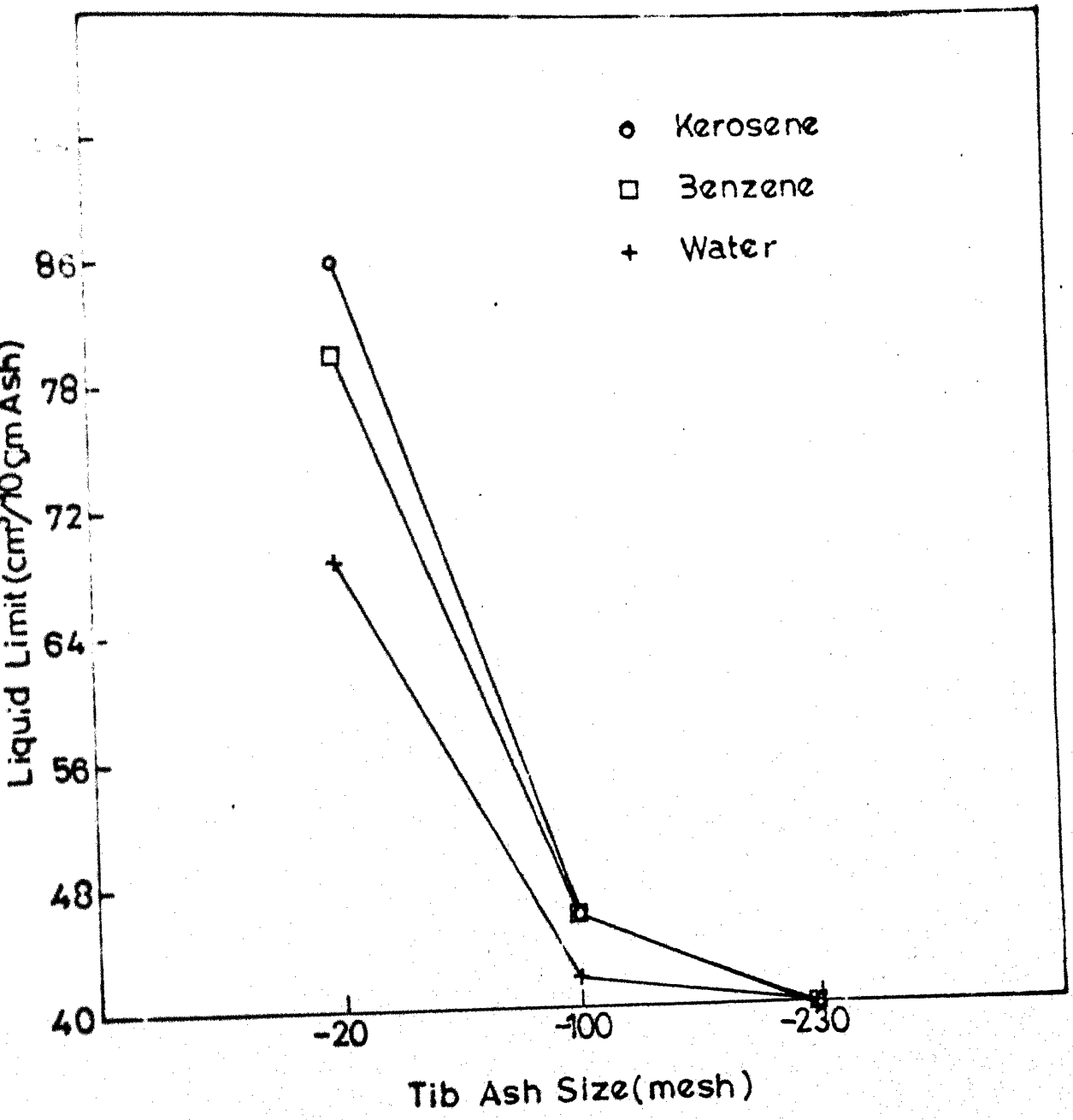
Kerosene
Benzene
Water
86
78
72
64
56
48
40
Liquid Limit (cm³/10gm Ash)
-20
-100
-230
Tib Ash Size(mesh)

Fig. 4.12

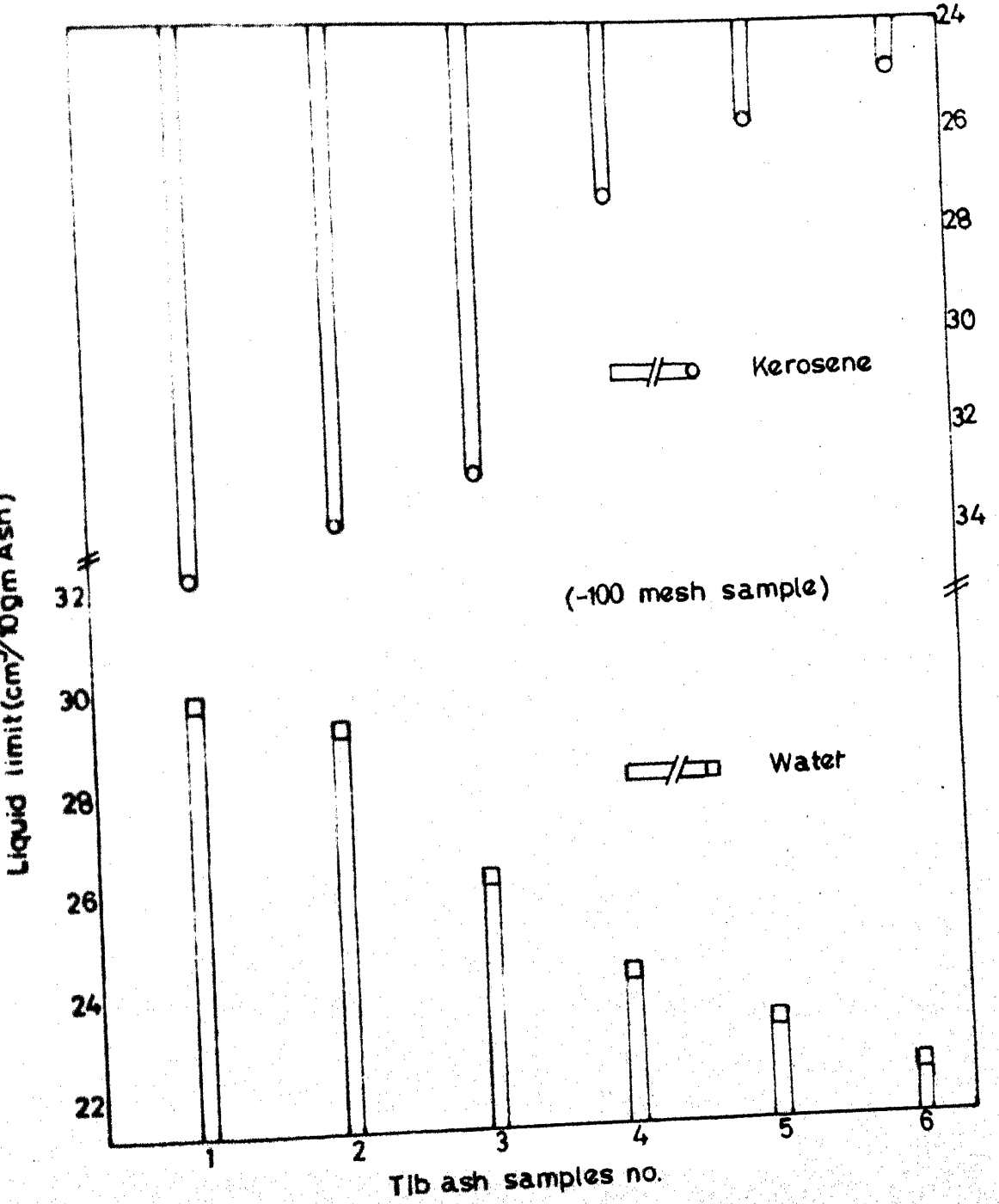
24
26
28
30
32
34
Kerosene
(-100 mesh sample)
Water
32
30
28
26
24
22
Liquid limit (cm³/10gm Ash)
1
2
3
4
5
6
Tlb ash samples no.

Fig. 413

CHAPTER 5

CONCLUSION

The following concluding remarks can be made on the basis of the experimental work carried out and results obtained therefrom.

- The variation in densities shows an increasing trend with increase in temperature of burning husk, consistent with the reduction in pore volume, porosity, surface area and the phase transformation of silica. The marked change observed over the temperature range 600-1000°C is reflected both in BET surface area and Hg porosimetry studies. This accounts for the formation of crystalline phases of silica as revealed by x-ray analysis.

- Cumulative pore volume, porosity and relative pore volume decrease with increase in temperature. There exists a bimodal distribution of pores, namely, one mode in the macroporous range 100 nm to 600 nm and the other in the mesoporous range 3 nm to 8 nm. The specific surface area decreases rapidly with increase in temperature due for the closing up of pores by sintering.

- The liquid limit trend of fired rice husk ash at various temperatures is consistent with x-ray, porosity and surface area trends. The abrupt drop in the liquid limit

between 600 and 1000°C is clearly revealed by x-ray, Hg-porosimetry and BET surface area studies. The liquid limit results for TIB ash samples are again consistent with the amount of crystalline phases detected by x-ray.

CHAPTER 6

SUGGESTIONS FOR FURTHER WORK

1. Electron Microscopy of rice husk ash fired at various temperatures can be studied. The actual size and shape of the pores obtained from the electron microscopy can be compared with Hg-porosimetry and physical adsorption studies.

2. A generalised mathematical model can be developed for the variation in pore size distribution as a function of temperature.

3. Solubilities of rice husk ash fired at various temperatures in sodium hydroxide can be carried out and can be compared with the liquid limits for rice husk ash reactivity.

APPENDIX

EXPERIMENTAL DATA AND CALCULATIONS

Table A.1. Variation in Tapped Bulk and Apparent true densities of rice husk ash with firing temperature.

Temperature (°C)	Tapped Bulk density (gm/cm^3)	Apparent true density (gm/cm^3)
450	0.2925	-
600	0.2777	1.970
800	0.3192	2.289
1000	0.3050	2.300
1200	0.3330	2.350
1400	0.3450	2.358

Table 1.2. BET Specific surface area of rice husk ash fired at various temperatures.

Temperature (°C)	Sp. surface area (m^2/gm)
400	60
600	76
800	4.8
1000	0.512
1200	0.302
1400	0.12

A.2. Porosimeter Data and Calculations

A.2.1 Pore volume :

(i) Sample : Rice Husk Ash fired at 800°C and pressed at 2500 psi (Pellet)

Cell factor ; 0.000784 cc/count

Weight of the sample = 1.0321 gm. W_s

A Applied pressure (psi)	B Corrected counter indication -	C Pore diameter for 130° contact angle (176.8÷A) (μm)	D Volume of pores of indicated dia and larger B(Factor ÷W_s) (cc/g)
15.35	0	11.518	- 0
52.148	49	3.390	0.037
100	66	1.768	0.050
400	321	0.442	0.244
550	351	0.321	0.266
600	358	0.295	0.272
1000	375	0.1768	0.285
5000	449	0.0354	0.341
7000	462	0.025	0.350
10000	464	0.0177	0.352
15000	466	0.0118	0.354
20000	474	0.0088	0.360
25000	477	0.007	0.362
30000	481	0.0059	0.365

(ii) Sample : Rice Husk Ash fired at 800°C and pressed at 5000 psi (pellet)

Cell factor : 0.000784 cc/count

Weight of the sample : 1.450 gm .

W_s

A	B	C	D
Applied pressure	Corrected counter indication	Pore diameter for 130° contact angle(176.8 ÷ A)	Volume of pores of indicated dia and larger B(Factor ÷ W_s)
(psi)	-	(μm)	(cc/gm)
1.2	0	147.3	0
2	2	88.4	0.001
5.2	2	34	0.001
6.2	2	28.52	0.001
7.25	2	24.34	0.001
8.25	2	21.43	0.001
10.2	5	17.34	0.0027
12.2	5	14.5	0.0027
14.25	5	12.40	0.0027
15.25	5	11.59	0.0027
16.2	9	10.92	0.0049
27.2	22	6.50	0.0119
47.2	33	3.75	0.0178
52.2	33	3.39	0.0178
100	65	1.768	0.0351
160	141	1.105	0.0762
180	170	0.982	0.0920
210	202	0.842	0.1092

350	288	0.505	0.1557
620	364	0.285	0.1968
700	368	0.253	0.1989
1000	386	0.177	0.2087
3000	458	0.059	0.2476
5000	482	0.0354	0.2606
10000	500	0.0177	0.2704
15000	515	0.0118	0.2785
20000	525	0.0088	0.2839
25000	538	0.007	0.2909
29000	542	0.006	0.2930

A.3. Porosimeter Data and Calculations

Cell factor = 0.000784 cc/count.

(iii) Sample : Rice Husk Ash fired at 600°C (powder)

Weight of the sample W_s : 1.300 gm.

A	B	C	D
Applied pressure (psi)	Corrected counter indication.	Pore diameter for 130° contact angle (176.8 ÷ A) (μm)	Volume of powder pores of Indicated dia and larger B (Factor ÷ W_s) (cc/gm)
19	0	9.305	0
26.29	33	6.720	0.02
66.24	159	2.670	0.096
81.23	197	2.180	0.119
171.2	295	1.032	0.178
200	318	0.884	0.192
250	331	0.707	0.200
300	348	0.589	0.210
315	348	0.560	0.210
400	364	0.442	0.220
430	364	0.410	0.220
500	383	0.350	0.231
525	391	0.337	0.236
595	398	0.297	0.240
650	398	0.27	0.240
1400	418	0.126	0.252

3000	434	0.059	0.263
5000	466	0.035	0.281
10000	486	0.018	0.293
15000	506	0.011	0.305
20000	529	0.009	0.319
25000	560	0.007	0.338
30000	585	0.006	0.353

- - - - - - - - - - - - - - - - -

(iv) Sample : Rice Husk ash fired at 800°C (powder)

Weight of the sample W_s = 1.10 gm.

A	B	C	D
Applied pressure	Corrected counter Indication	Pore diameter for 130° contact angle (176.8 ÷ A)	Volume of powder pores of indicated dia and larger B (Factor ÷ W_s)
(psi)		(μm)	(mc/gm)
30	25	5.893	0.018
50	58	3.536	0.041
100	108	1.768	0.077
200	138	0.884	0.098
500	144	0.354	0.103
1000	168	0.177	0.120
5000	175	0.0354	0.125
10000	182	0.0177	0.130
30000	217	0.006	0.155

- - - - - - - - - - - - -

V. Sample : Rice husk ash fired at 1000°C (powder)

Weight of the sample W_s = 0.95 gm

A Applied pressure (psi)	B Corrected counter indication	C Pore diameter for 130° contact angle (176.8 ÷ A) (μm)	D Volume of pores of indicated diameter and larger B(Factor ÷ W_s) (cc/gm)
21.9	0	8.064	0
101.9	61	2.642	0.05
250	73	0.702	0.06
500	73	0.352	0.06
1000	97	0.177	0.08
5000	97	0.035	0.08
10000	97	0.018	0.08
15000	97	0.012	0.08
20000	99	0.009	0.082
25000	101	0.007	0.083
30000	101	0.006	0.083

- - - - - - - - - - - - -

VI. Sample Husk ash fired at 1200 °C (powder)

Weight of the sample W_s = 1.185 gm.

Applied pressure (psi)	Corrected counter indication	Pore diameter for 130° contact angle(176.8 ÷ A) (µm)	Volume of powder pores of indicated dia and larger B (Factor ÷ W_s) (cc/gm)
46.12	42	3.750	0.028
56.1	53	3.152	0.035
160	71	1.105	0.047
250	73	0.702	0.048
400	73	0.44	0.048
600	86	0.295	0.057
775	92	0.228	0.061
1000	94	0.177	0.062
5000	94	0.035	0.062
10000	95	0.018	0.063
15000	97	0.012	0.064
20000	98	0.009	0.065
25000	98	0.007	0.065
30000	98	0.006	0.065

A.3.2 Pore size distribution

(i) Sample : 600°C fired Rice husk ash powder

P psi	r μm	$\frac{dv}{dp}$	D(r)
46	1.922	1.9×10^{-3}	0.046
73.5	1.203	1.5×10^{-3}	0.094
126	0.702	6.55×10^{-4}	0.118
185.5	0.476	2.76×10^{-4}	0.188
225	0.393	1.6×10^{-4}	0.092
275	0.321	2×10^{-4}	0.170
307.5	0.288	0	0
357.5	0.247	1.10×10^{-4}	0.170
415	0.213	0	0
465	0.190	1.57×10^{-4}	0.385
512.5	0.1725	2×10^{-4}	0.594
560	0.158	5.7×10^{-5}	0.203
622.5	0.142	0	0
1025	0.086	1.6×10^{-5}	0.191
2200	0.04	6.88×10^{-6}	0.378
4000	0.022	8.5×10^{-6}	1.539
7500	0.012	2.4×10^{-6}	1.50
12500	0.007	2.4×10^{-6}	4.29
17500	0.005	2.8×10^{-6}	9.80
22500	0.004	3.8×10^{-6}	21.92
27500	0.003	3×10^{-6}	25.8

(ii) Sample : 800°C fired Rice husk ash powder

P psi	r μm	$\frac{dv}{dp}$	D(r)
40	2.209	1.15×10^{-3}	0.021
75	1.180	7.2×10^{-4}	0.046
150	0.590	2.1×10^{-4}	0.053
350	0.253	1.66×10^{-5}	0.023
750	0.118	3.4×10^{-5}	0.216
3000	0.030	1.25×10^{-6}	0.127
7500	0.012	1.0×10^{-6}	0.636
20000	0.004	1.25×10^{-6}	5.682

(iii) Sample : 1000°C fired rice husk ash powder

P psi	r μm	$\frac{dv}{dp}$	D(r)
61	1.450	6.25×10^{-4}	0.025
175	0.505	6.71×10^{-5}	0.0233
375	0.236	0	0
750	0.120	4.0×10^{-5}	0.25
3000	0.030	0	0
7500	0.012	0	0
12500	0.007	0	0
17500	0.005	4.0×10^{-7}	1.4
22500	0.004	2.0×10^{-7}	1.154
27500	0.003	0	0

(iv) Sample : 1200°C fired rice husk ash powder.

p	r	$\frac{dv}{dp}$	D(r)
psi	µm		
50	1.768	7×10^{-4}	0.020
107.5	0.820	1.14×10^{-4}	0.015
205	0.430	1.11×10^{-5}	0.005
325	0.270	0	0
500	0.176	4.5×10^{-5}	0.178
687.5	0.129	2.29×10^{-5}	0.123
887.5	0.100	3.08×10^{-6}	0.027
3000	0.029	0	0
7500	0.012	2×10^{-7}	0.125
12500	0.007	2×10^{-7}	0.357
17500	0.005	0	0
22500	0.004	0	0
27500	0.003	0	0

- - - - - - - - - - - - - - -

Table A.4.2 Liquid limits of different sized TIB Ash samples.
Weight of rice husk ash = 20 gms.

Size (Mesh)	Water limit cm^3	Kerosene limit cm^3	Benzene limit cm^3
-20 (-850 µm)	59	86	80
-100 (-150 µm)	42	46	46
-230 (-63 µm)	40	40.5	40.5

Table A.4.3 Liquid limits of TIB ash samples
Weight of rice husk ash = 10 gms
size - 100 mesh (-150 µm)

Sample No.	Water limit (cm^3)	Kerosene limit (cm^3)
1	30.5	34
2	30	33
3	27	32
4	25	26.5
5	24	25
6	23	24

REFERENCES

1. V. Vijaya Bhaskar, "Development of High temperature thermal insulations using two waste materials : Thermit Slag and Rice husk ash", M.Tech. Thesis, Dept. of Metallurgical Engg., I.I.T., Kanpur, July, 1981.

2. P.K. Mehta, "The Chemistry and Technology of cements made from rice husk ash" Escap Workshop on production of cement like materials, Malayasia, October, 1979.

3. P.C. Kapur, Indian patent No. 142966 of December 1, 1975.

4. P.C. Kapur and A.S.R. Sai, "Ashment Cement" Internal report, I.I.T., Kanpur.

5. P.C. Kapur, "Thermal Insulations from rice husk ash, an agricultural waste", Ceramurgia Inst. Vol.6, No.2, 1980, p.75.

6. June-Gunn Lee and Ivan B. Cutler,"Formation of Silicon carbide from rice hulls." American Ceramic Society Bulletin, Vol. 54, No.2, 1975, p.195.

7. H.D. Banerjee, S. Sen and H.N. Acharaya, "Investigation on the production of silicon from rice husks by the magnesium method", Material Science and Engineering, Vol. 52, 1982, p. 173.

8. P.K. Basu, C.J. King and S. Lynn, AIChE Journal Vol. 19, 1973, p. 439.

9. Hanafi and S.A. Abo-El Enein, "Surface properties of silicas produced by thermal treatment of rice husk ash", Thermo Chimica Acta, Vol. 37, 1980, pp. 307-143.

10. D.M. Ibrahim, S.A. El-Hemaly and F.M. Abdelkerim, "Study of rice husk ash silica by infra red spectroscopy," Thermochimica Acta, Vol 37, 1980, pp. 307-314.

11. E.W. Washburn, Proc. Natl. Acad. Sci. US, 7 (1921), 115.

12. A.J. Goodsel, "Mercury penetration porosimetry in analysis of exhaust catalysts and catalyst supports". Powder Technology, Vol. 9, 1974, pp. 191-197.

13. G.P. Androutsopoulos and E.T. Woodburn, "Macropore structure of a low rank coal and its froath flotation fractions". Power Technology, Vol.33, 1982, pp.175-186.

14. S. Raghavan and D.W. Fuerstenau "Characterization and pore structure analysis of a copper ore containing chrysocolla" "International Journal of Mineral Processing, Vol.4, 1977, pp. 381-394.

15. O.J. Whittemore Jr. and J.J. Sipe "Pore Growth during the initial stages of sintering ceramics" Powder Technology, Vol. 9, 1974, pp.154-164.

16. J.A. Lee and W.C. Maskell, "A study of the Inter and Intra fibre pore characteristics of some nylon fabrics by mercury porosimetry powder technology", vol. 9, 1974, pp.165-171.

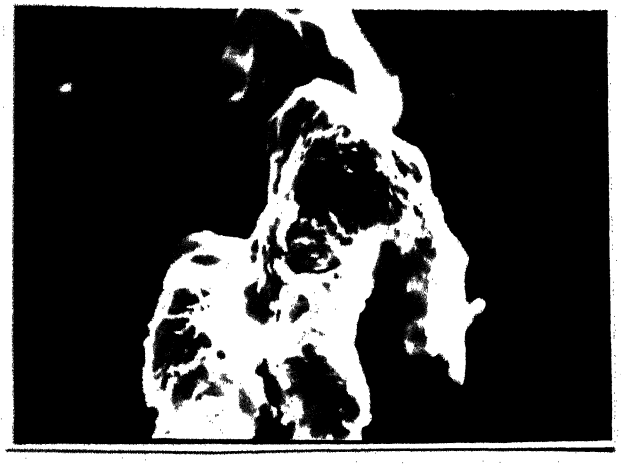

600°C fired Ash Sample

1200°C fired Ash Sample

SEM Photograph of Rice husk Ash.

ME-1983-M-MAN-CHA